EUROPEAN ORGANIZATION FOR NUCLEAR RESEARCH (CERN)

CERN-EP-2024-049
2024/03/05

CMS-EXO-22-015

Search for new physics with emerging jets in proton-proton collisions at $\sqrt{s} = 13\,\text{TeV}$

The CMS Collaboration*

Abstract

A search for "emerging jets" produced in proton-proton collisions at a center-of-mass energy of 13 TeV is performed using data collected by the CMS experiment corresponding to an integrated luminosity of 138 fb^{-1}. This search examines a hypothetical dark quantum chromodynamics (QCD) sector that couples to the standard model (SM) through a scalar mediator. The scalar mediator decays into an SM quark and a dark sector quark. As the dark sector quark showers and hadronizes, it produces long-lived dark mesons that subsequently decay into SM particles, resulting in a jet, known as an emerging jet, with multiple displaced vertices. This search looks for pair production of the scalar mediator at the LHC, which yields events with two SM jets and two emerging jets at leading order. The results are interpreted using two dark sector models with different flavor structures, and exclude mediator masses up to 1950 (1850) GeV for an unflavored (flavor-aligned) dark QCD model. The unflavored results surpass a previous search for emerging jets by setting the most stringent mediator mass exclusion limits to date, while the flavor-aligned results provide the first direct mediator mass exclusion limits to date.

Submitted to the Journal of High Energy Physics

*See Appendix A for the list of collaboration members

1 Introduction

Although there is a preponderance of evidence from astronomical and cosmological observations [1–5] for the existence of dark matter (DM), it has not yet been detected in laboratories, suggesting that its origin may be associated with as-of-yet unobserved physics processes beyond the standard model (SM). As experimental searches have excluded a large portion of the phase space of DM models with weakly interacting massive particles, alternative theoretical models have been developed with a hidden gauge sector, similar to quantum chromodynamics (QCD), which can result in strongly self-interacting DM particles [6–9]. Dark matter of this type could interact with SM particles through so-called mediator particles and potentially be produced at colliders, producing signatures such as semivisible jets [10] or emerging jets (EJs) [11].

The search described in this paper is motivated by the models proposed in Refs. [11–13]. A composite dark sector, which has a QCD-like non-Abelian gauge symmetry SU($N_{\text{color}}^{\text{dark}}$), where $N_{\text{color}}^{\text{dark}}$ is the number of dark colors, is added to the SM gauge group. We consider the case where fermions in the dark sector (dark quarks Q_{dark}) communicate with the SM quarks through a scalar mediator X_{dark}, which is charged under both SM QCD and dark QCD and which couples to a quark and a dark quark via Yukawa interactions with coupling strength $\kappa_{\alpha i}$, where the subscript α (i) denotes flavors of dark (SM) quarks. The mediator can be pair produced through gluon splitting at the LHC, similar to the pair production of a single type of squark in supersymmetry [14]. In fact, the production cross section is the same as for pair production of right-handed top squarks [15, 16] multiplied by $N_{\text{color}}^{\text{dark}}$. Each mediator decays into a quark and a dark quark, as shown in Fig. 1. The dark quarks hadronize into dark hadrons. Of the dark hadrons, either the lightest dark baryon or dark meson is stable and therefore a good DM candidate, escaping the detector without leaving a signal. The unstable dark hadrons have lifetimes and branching fractions to SM particles that depend on the masses of the dark mesons, the mediator mass, the coupling strength $\kappa_{\alpha i}$, along with phase-space and spin considerations.

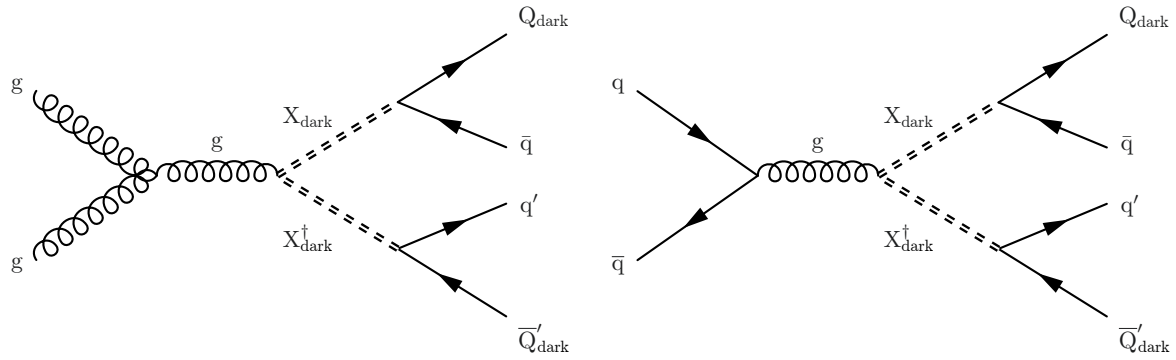

Figure 1: Feynman diagrams for pair production of dark mediator particles via gluon-gluon fusion (left) and quark-antiquark annihilation (right), with each mediator decaying to an SM quark and a dark quark.

The first version of this model that we consider, referred to as "unflavored", has a simplified flavor structure in the coupling of the dark sector to SM particles, such that only the Yukawa coupling to the d quark is non-negligible [11]. Equation (1), taken from Ref. [11], gives the average decay length of a dark pion in this model:

$$c\tau_{\pi_{\text{dark}}} = 80\,\text{mm}\left(\frac{1}{\kappa^4}\right)\left(\frac{2\,\text{GeV}}{f_{\pi_{\text{dark}}}}\right)^2\left(\frac{100\,\text{MeV}}{m_{\text{d}}}\right)^2\left(\frac{2\,\text{GeV}}{m_{\pi_{\text{dark}}}}\right)\left(\frac{m_{\text{X}_{\text{dark}}}}{1\,\text{TeV}}\right)^4, \tag{1}$$

where κ is the coupling between dark quarks and the SM down quark, $f_{\pi_{\text{dark}}}$ is the dark pion decay constant, m_{d} is the mass of the SM down quark, and $m_{\pi_{\text{dark}}}$ is the dark pion mass.

If instead multiple Yukawa couplings $\kappa_{\alpha i}$ have non-negligible values, the average decay length for dark mesons composed of dark quarks of flavor indices α and β is given by Eq. (2) from Ref. [13]:

$$c\tau^{\alpha\beta}_{\pi_{\text{dark}}} = \frac{8\pi m^4_{\text{X}_{\text{dark}}}}{N_{\text{c}} m_{\pi_{\text{dark}}} f^2_{\pi_{\text{dark}}} \sum_{i,j} |\kappa_{\alpha i}\kappa^*_{\beta j}|^2 \left(m_i^2 + m_j^2\right) \sqrt{\left(1 - \frac{(m_i + m_j)^2}{m^2_{\pi_{\text{dark}}}}\right)\left(1 - \frac{(m_i - m_j)^2}{m^2_{\pi_{\text{dark}}}}\right)}}, \quad (2)$$

where $m_{\text{X}_{\text{dark}}}$ is the mediator particle mass, N_{c} is the SM color factor, and m_i, m_j are the masses of the SM quarks with flavor indices i, j, respectively. Within this model, we focus on the "flavor-aligned" scenario, with three dark quark flavors that couple to the SM down-type quarks (d, s, b) via a diagonal matrix $\kappa_{\alpha i} = \kappa_0 \delta_{\alpha i}$. Because of spin considerations, dark hadron decays to heavier SM particles are favored, typically resulting in a large number of b quarks in the decays when kinematically allowed. We characterize the flavor-aligned model in terms of the maximum lifetime for any dark pion, $c\tau^{\text{max}}_{\pi_{\text{dark}}}$. When the lifetimes are long enough to give macroscopic decay distances, the resulting signature from either model is two SM jets and two EJs containing multiple displaced vertices. Alternative dark sector models with short dark hadron lifetimes can produce "semivisible" jets that each contain a mixture of promptly produced SM particles and invisible DM particles.

Previous experimental searches for strongly self-interacting DM have been made using proton-proton (pp) collision data collected at the CERN LHC at $\sqrt{s} = 13\,\text{TeV}$ and corresponding to about $140\,\text{fb}^{-1}$. This includes a search for semivisible jets by the CMS Collaboration [17], a search for semivisible jets by the ATLAS Collaboration [18], and a search for dark quarks in a dijet final state by ATLAS [19]. In addition, a previous search for EJs interpreted with an unflavored dark sector model was performed by the CMS Collaboration using a data sample collected in 2016, corresponding to an integrated luminosity of $16.1\,\text{fb}^{-1}$ [20].

In this paper, we present a search for the emerging jet signatures of the unflavored and the flavor-aligned dark sector models, using the data set collected by the CMS Collaboration in 2016–2018 using pp collisions at a center-of-mass energy of 13 TeV and corresponding to $138\,\text{fb}^{-1}$. The search strategy first identifies EJs by exploiting their topological differences relative to SM jets using selection criteria optimized separately for each model. Then, the probability for an SM jet to be misidentified as an EJ is measured, and the background is estimated using control samples in data. The main background comes from SM multijet production where SM jets are misidentified as EJs.

Compared to the previous analysis [20], we have extended the unflavored EJ model search to a wider parameter space. This study also includes the first dedicated search for a flavored dark QCD sector. We have implemented a number of important changes that considerably increase the sensitivity of the search, including the incorporation of a novel machine learning (ML) technique, which significantly enhances the EJ identification (tagging) performance. The tabulated results are provided as a HEPData record [21].

This paper is organized as follows. In Section 2 we give an introduction of the CMS detector, followed in Section 3 by a detailed description of the simulated data used in this search. The event reconstruction and triggering algorithms are discussed in Section 4. In Section 5 we present the analysis strategy, two independent EJ tagging methods, and the background

estimation method. The treatment of uncertainties is detailed in Section 6. The results are presented in Section 7 and summarized in Section 8.

2 The CMS detector

The central feature of the CMS apparatus is a superconducting solenoid of 6 m internal diameter, providing a magnetic field of 3.8 T. Located within the solenoid volume are a silicon pixel and strip tracker, a lead tungstate crystal electromagnetic calorimeter (ECAL), and a brass and scintillator hadron calorimeter (HCAL), each composed of a barrel and two endcap sections. Forward calorimeters extend the pseudorapidity (η) coverage provided by the barrel and endcap detectors. Muons are measured in gas-ionization detectors embedded in the steel flux-return yoke outside the solenoid.

The silicon tracker used in 2016 measured charged particles within the range $|\eta| < 2.5$. For nonisolated particles of $1 < p_T < 10$ GeV and $|\eta| < 1.4$, the track resolutions were typically 1.5% in p_T and 25–90 (45–150) μm in the transverse (longitudinal) impact parameter d_{xy} (d_z) [22]. At the start of 2017, a new pixel detector was installed [23]; the upgraded tracker measured particles up to $|\eta| < 3.0$ with typical resolutions of 1.5% in p_T and 20–75 μm in d_{xy} for nonisolated particles of $1 < p_T < 10$ GeV [24].

Physics events of interest are selected using a two-tiered trigger system. The first level, called the level-1 trigger, is composed of custom hardware processors and uses information from the calorimeters and muon detectors to select events at a rate of around 100 kHz within a fixed latency of about 4 μs [25]. The second level, known as the high-level trigger, consists of a farm of processors running a version of the full event reconstruction software optimized for fast processing, and reduces the event rate to around 1 kHz before data storage [26]. A more detailed description of the CMS detector, together with a definition of the coordinate system used and the relevant kinematic variables, can be found in Ref. [27].

3 Event simulation

Monte Carlo (MC) events are used to evaluate the signal acceptance, optimize selection criteria, and test the closure of the background estimation methods.

The signal process is generated using the Hidden Valley module [28, 29] in PYTHIA version 8.240 [30], based on Ref. [11]. In the unflavored scenario, we choose the number of mass degenerate dark quark flavors to be $N_{\text{flavor}}^{\text{dark}} = 7$, following Ref. [11]. The running of the dark coupling constant with Q^2, where Q is the momentum transfer, is faster for smaller $N_{\text{flavor}}^{\text{dark}}$, and the resulting showers have fewer dark mesons. In the flavor-aligned scenario, $N_{\text{flavor}}^{\text{dark}} = 3$ is used, and $\kappa_{\alpha i}$ is set to be diagonal, with all diagonal elements having the value κ_0. For this scenario, the PYTHIA Hidden Valley module is modified to produce the different dark hadron species at the desired occurrence frequencies based on the dark quark flavors. For both cases, we consider a representation similar to QCD with $N_{\text{color}}^{\text{dark}} = 3$. The dark quark masses are degenerate and equal to the confinement scale Λ_{dark}. The dark pion mass is set to be half of Λ_{dark}, and the dark ρ meson mass four times the dark pion mass. The natural width of X_{dark} is set to 10 GeV, a relatively small value compared to the detector resolution. Under these assumptions, the free parameters of the model are limited to the mediator mass $m_{X_{\text{dark}}}$, the dark pion mass $m_{\pi_{\text{dark}}}$, and the dark pion lifetime $c\tau_{\pi_{\text{dark}}}$. Tables 1 and 2 summarize the signal model parameters used in this search. The signal cross section, described in Section 1, is computed at next-to-leading order (NLO), with the resummation of soft gluon emission included at next-to-

leading-logarithmic accuracy.

Table 1: Model parameters for the unflavored model.

Model parameter	List of values
$m_{\mathrm{X}_{\mathrm{dark}}}$ [GeV]	1000, 1200, 1400, 1500, 1600, 1800, 2000, 2200, 2400, 2500
$m_{\pi_{\mathrm{dark}}}$ [GeV]	10, 20
$c\tau_{\pi_{\mathrm{dark}}}$ [mm]	1, 2, 5, 25, 45, 60, 100, 150, 225, 300, 500, 1000

We simulate SM QCD multijet events and γ+jets events using the MADGRAPH5_aMC@NLO 2.6.5 event generator [31] at leading order with the MLM matching procedure [32].

In all cases parton showering and hadronization is performed using PYTHIA8 with the CP5 underlying event tune [33] and the NNPDF3.1 next-to-NLO parton distribution functions (PDFs) [34]. The response of the CMS detector is modeled using GEANT4 [35], and corrections are applied to the simulated samples to account for the differences in resolutions and efficiencies between the data and the simulation.

4 Event reconstruction and triggering

A global "particle-flow" (PF) algorithm [36] aims to reconstruct all individual particles in an event, combining information provided by the tracker, calorimeters, and muon system. The reconstructed information from the different subsystems is used to build physics objects such as photons, leptons, jets, and missing transverse momentum [37–39].

Jets are reconstructed from the PF particles using the anti-k_{T} algorithm [40, 41] with a distance parameter of 0.4. The jet momentum (energy) is calculated as the vectorial (scalar) sum of the momenta (energies) of all clustered particles. Corrections derived from data and simulation are applied to the jet energy. Jets that are consistent with the fragmentation of b quarks (b jets) are identified using the DEEPJET discriminator [42–44]. Both the medium and loose working points are used; the medium (loose) working point has an 85% (90%) probability of correctly identifying b jets with $p_{\mathrm{T}} > 90\,\mathrm{GeV}$ and a 1% (10%) probability of misidentifying light-flavor jets as b jets. The scalar p_{T} sum of all jets within an event (H_{T}) is used to select energetic events.

The pp interaction vertices are reconstructed by clustering tracks on the basis of their z coordinates along the beamline at their points of closest approach to the beam axis using a deterministic annealing algorithm [45]. The position of each vertex is estimated with an adaptive vertex fit [46].

Multiple vertex candidates can be reconstructed because of additional pp interactions in a bunch crossing (pileup). The primary vertex (PV) is taken to be the vertex corresponding to the hardest scattering in the event, evaluated using tracking information alone, as described in Section 9.4.1 of Ref. [47]. The contribution from charged-particle tracks from pileup interactions is reduced by rejecting those associated with other vertices [48]. The PV is required to be within 15 cm of the CMS detector center in the z direction to ensure optimal reconstruction efficiency.

The analysis considers data collected using triggers based on jet p_{T} and on H_{T} calculated from the summed p_{T} of online-reconstructed jets. The trigger used for the data collected in 2016 requires at least one jet with $p_{\mathrm{T}} > 450\,\mathrm{GeV}$ or $H_{\mathrm{T}} > 900\,\mathrm{GeV}$, while for 2017–2018, the H_{T} threshold is increased to 1050 GeV and there is no p_{T} requirement. The inclusion of a jet p_{T} trigger requirement for 2016 was necessary because, in part of the 2016 data taking period, some

Table 2: Parameters used for the flavor-aligned model. In order to probe a range of lifetimes, the values of κ_0 listed in columns 3–7 are tuned to give the desired $c\tau^{\text{max}}_{\pi_{\text{dark}}}$ values of 5, 25, 45, 100, and 500 mm. In addition, samples were made with fixed $\kappa_0 = 1$, with a resultant value of $c\tau^{\text{max}}_{\pi_{\text{dark}}}$ that depends on the other model parameters.

$m_{\text{X}_{\text{dark}}}$ [GeV]	$m_{\pi_{\text{dark}}}$ [GeV]	κ_0 value				
1000	6	0.92	0.61	0.53	0.43	0.29
	10	0.62	0.42	0.36	0.30	0.20
	20	0.37	0.25	0.21	0.18	0.12
1200	6	1.10	0.73	0.63	0.52	0.35
	10	0.75	0.50	0.43	0.35	0.24
	20	0.45	0.30	0.26	0.21	0.14
1400	6	1.28	0.86	0.74	0.61	0.41
	10	0.87	0.58	0.50	0.41	0.28
	20	0.52	0.35	0.30	0.25	0.16
1600	6	1.47	0.98	0.85	0.69	0.46
	10	1.00	0.67	0.58	0.47	0.32
	20	0.59	0.40	0.34	0.28	0.19
1800	6	1.65	1.10	0.95	0.78	0.52
	10	1.12	0.75	0.65	0.53	0.36
	20	0.67	0.45	0.39	0.32	0.21
2000	6	1.83	1.23	1.06	0.87	0.58
	10	1.25	0.84	0.72	0.59	0.40
	20	0.74	0.50	0.43	0.35	0.23
2200	6	2.02	1.35	1.16	0.95	0.64
	10	1.37	0.92	0.79	0.65	0.43
	20	0.82	0.55	0.47	0.39	0.26
2400	6	2.20	1.47	1.27	1.04	0.70
	10	1.50	1.00	0.87	0.71	0.47
	20	0.89	0.60	0.51	0.42	0.28
2500	6	2.29	1.53	1.32	1.08	0.72
	10	1.56	1.04	0.90	0.74	0.49
	20	0.93	0.62	0.54	0.44	0.29

jets reaching the saturation energy for the level-1 trigger were mistakenly dropped from the H_{T} sum, resulting in a significant loss of efficiency. This loss was recovered by including the single-jet trigger requirement. The H_{T} threshold was increased in 2017 to compensate for the higher instantaneous luminosity. The efficiencies for an event to pass any of these trigger conditions in both data and simulation are measured from data sets collected with an independent trigger that requires a muon with $p_{\text{T}} > 50\,\text{GeV}$. In both cases, the efficiencies are close to unity above the signal selection H_{T} thresholds, and the difference between the efficiencies as measured in simulation and data is applied as a correction to the simulation.

5 Analysis

The offline analysis selects energetic events with at least four jets. Jets are classified as EJ candidates using information from tracks associated with the jets. An overview of the event selection strategy is given in Section 5.1. Descriptions of the "candidate" EJ identification criteria ("tagging") is given in Section 5.2. The algorithms used to optimize the selection criteria to maximize signal sensitivity, and the resulting event selection requirements are described in Section 5.3. Section 5.4 describes the procedure used to estimate the background from control regions in data.

5.1 Event and physics object selection

While some SM hadrons, such as those containing b quarks, have macroscopic decay lengths, tracks associated with SM jets mainly come from particles produced promptly (close to the collision primary vertex). In EJs, when the lifetime of one or more of the dark mesons is long, a substantial fraction of the tracks can emerge from displaced vertices. In addition, in the flavor-aligned scenario, most of the dark pion decay products are b quarks, which results in displaced tracks even when the dark pion decays immediately. We use as our displacement measure the d_{xy} (d_z), measured from the PV to the point of closest approach on the track trajectory, as this gives better sensitivity than reconstructing individual decay vertices. Jets used in this analysis are required to have $p_{\mathrm{T}} > 100\,\mathrm{GeV}$, as we are looking for EJs originating from a heavy-mediator decay, and $|\eta| < 2$, to ensure that they are well contained in the tracker. Jet candidates are also required to pass a set of quality criteria to reject spurious jets from instrumental sources [49]. High-purity tracks, as defined in Ref. [22], with $p_{\mathrm{T}} > 1\,\mathrm{GeV}$ are associated with jets by requiring the angular separation between the jet direction and the track direction, $\Delta R = \sqrt{(\Delta\eta)^2 + (\Delta\phi)^2} < R_{\mathrm{max}}$, where $\Delta\eta$ is the η separation between the jet and the track, and $\Delta\phi$ is the separation in the azimuthal direction. We also reject tracks with $|d_z| > d_z^{\mathrm{max}}$ to suppress jets from pileup interactions. The values of R_{max} and d_z^{max} are optimized for each signal model. If a track can be assigned to multiple jets, it is assigned to the jet with the smallest ΔRseparation. Jets are required to have at least one associated track so that the jet displacement measure can be calculated. To suppress events with a poorly reconstructed PV, we require that at least 10% of associated tracks have a longitudinal displacement from the PV less than 0.01 cm.

Candidate signal events are required to have high H_{T} and at least four jets passing the criteria above. At least two of these four jets must be tagged as EJs. If more than four jets are found, the four jets with the largest p_{T} are used. The H_{T} and EJ criteria are optimized for each signal model.

5.2 EJ tagging

Two EJ tagging strategies are used in this analysis. The first selects candidate EJs via requirements on jet-level variables using track displacement measures ("model-agnostic selection"). The second uses a graph neural network trained on specific signal models to determine an EJ tagging score ("machine learning or ML-based selection"). The model-agnostic method allows for a simpler reinterpretation of the results for alternate theoretical models not considered in this paper, while the ML-based approach achieves the best possible sensitivity for the specific models studied here.

The model-agnostic EJ tagger uses different input features for the unflavored and flavor-aligned dark sector models, while the ML-based EJ tagger is trained separately for each class of model.

5.2.1 Model-agnostic EJ tagging

For the EJ tagging that targets the unflavored dark-sector models, $R_{\text{max}} = 0.4$ is used. The following variables, which were also used in Ref. [20], are used for the EJ tagging:

- $\left\langle d_{xy} \right\rangle$: this is the median d_{xy} of tracks associated with a jet.
- α_{3D}: this is defined as

$$\alpha_{\text{3D}} = \frac{\sum_{D_N < D_N^{\text{max}}} p_{\text{T}}^{\text{track}}}{\sum p_{\text{T}}^{\text{track}}},$$

  which is the ratio between the scalar p_{T} sum of the associated tracks with a pseudo-significance D_N smaller than the selection value D_N^{max} and the scalar p_{T} sum of all the associated tracks. The pseudo-significance D_N is defined as:

$$D_N = \sqrt{\left(\frac{d_z}{0.01\,\text{cm}}\right)^2 + \left(\frac{d_{xy}}{\sigma(d_{xy})}\right)^2},$$

  where $\sigma(d_{xy})$ is the d_{xy} uncertainty calculated from the covariance matrix of the fitted track trajectory. The d_z significance is based on the PV z resolution.

The distributions of these variables are presented in Fig. 2 for data events and for simulated signal and multijet background events. The data and simulated events shown require $H_{\text{T}} > 1200\,\text{GeV}$ and at least four jets with $p_{\text{T}} > 100\,\text{GeV}$ and $|\eta| < 2$, which is much less restrictive than the final signal selection requirements.

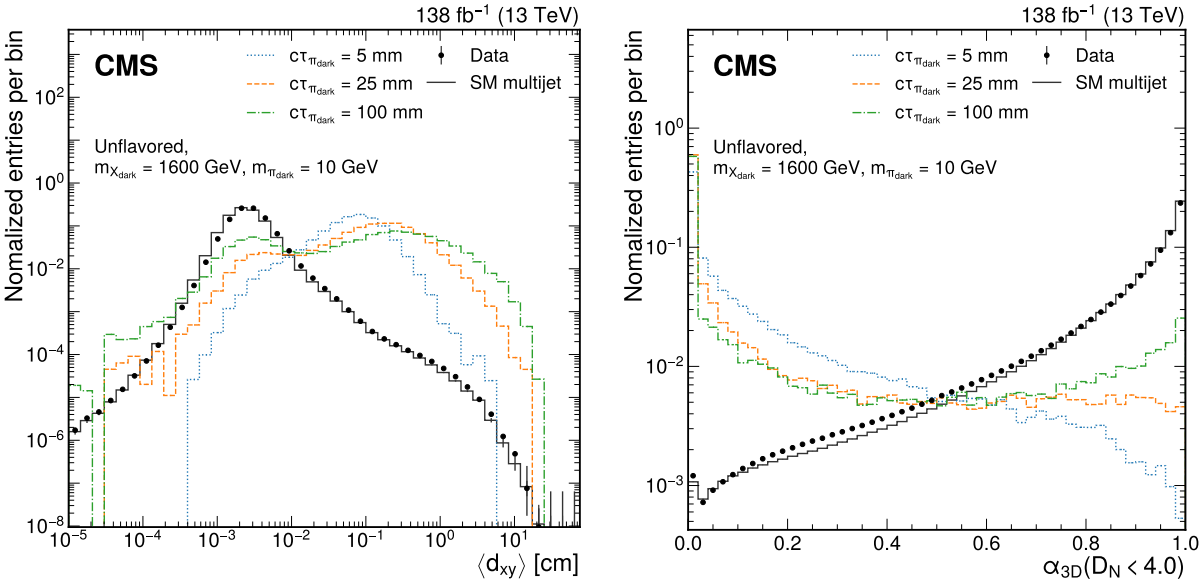

Figure 2: Distributions of the jet variables $\left\langle d_{xy} \right\rangle$ (left) and α_{3D} with $D_N^{\text{max}} = 4$ (right) used for the model-agnostic EJ tagging that targets the unflavored dark sector models are shown for data (points), SM multijet simulation (gray line), and signal jets in simulation (colored lines). The sums of the entries are normalized to unity.

The flavor-aligned dark-sector model has three different dark meson lifetime ranges: long-lived dark mesons (up to 50 cm for the κ_0 parameters considered in this search), dark mesons with a b-hadron-like displacement from prompt dark meson decays into b quarks, and dark mesons that decay promptly into light SM quarks. In addition, since at least one dark quark in the

flavor-aligned model couples to the b quark, the jets often contain heavy-flavor hadrons, and the resulting EJ is wider than that of the unflavored model. Because of this, the tagging of EJs in the flavor-aligned model associates tracks with a jet using a proximity measure of $R_{\text{max}} = 0.8$. The selection for candidate flavor-aligned EJs is based on the following variables:

- $n_{\text{track}}^{d_{xy}>d_{xy}^{\text{min}}}$, the number of tracks with d_{xy} greater than a threshold d_{xy}^{min}: this quantity exploits the tendency of the flavor-aligned dark sector to generate multiple long-lived SM mesons in the particle shower, resulting in a large number of displaced tracks.
- Jet girth: this is defined as the p_{T}-weighted ΔRseparation of tracks from the jet direction:

$$\text{Jet girth} = \frac{\sum_i p_{\text{T}}^i \Delta R(i, \text{jet})}{\sum_i p_{\text{T}}^i},$$

  where the index i runs over all tracks associated with the jet of interest. This variable exploits the feature that particles in EJs tend to have a wider angular separation than SM jets because of the large mass of the dark mesons.

Figure 3 shows the distributions of the tagging variables used in the flavor-aligned analysis for data, simulated signal, and multijet background events. The data and simulated events follow the same requirements as those appearing in Fig. 2.

As the jet-track association radius $R_{\text{max}} = 0.8$ is larger than the $R = 0.4$ value used to perform jet clustering, jets that have nearby soft jets can be misidentified as EJs. To remove these candidates, a modified N-subjettiness variable $\overline{\tau}_n$ is calculated as follows:

1. For each of the four candidate high-p_{T} jets, we consider all jets within $\Delta R < 0.8$ of the selected jets that have $p_{\text{T}} > 30\,\text{GeV}$ in decreasing order of jet p_{T}. These will be used as the "subjet" collection to calculate $\overline{\tau}_n$. Using this definition, all candidate jets will have at least one subjet: the candidate jet itself.

2. After determining the subjet collection assigned to each candidate jet, the computation of $\overline{\tau}_n$ is then carried out up to the leading n subjets:

$$\overline{\tau}_n = \frac{\sum_i p_{\text{T}}^i \min\{\Delta R_{ij}\}}{\sum_i 0.8 p_{\text{T}}^i},$$

   similar to the definition of the original N-subjettiness [50]. The index i runs over the tracks associated with the candidate jet, and j runs from 1 up to n for the subjet collection assigned to the selected jet.

The requirement that $\overline{\tau}_{2/1} = \overline{\tau}_2/\overline{\tau}_1 > 0.5$ is applied to all EJ candidates and is found to reliably suppress the misidentification of SM jets with nearby soft jets as EJs.

5.2.2 The ML-based EJ tagging

The ML-based tagger uses a graph neural network (GNN) based on PARTICLENET [51] to directly incorporate the track information. Two separate GNNs are trained to classify EJs: one for the unflavored model (uGNN) and the other for the flavor-aligned model (aGNN). Each is trained using all of the samples from its class of model, weighted equally. A validation data set is used to monitor potential bias and overtraining. The output of each GNN is a score ranging from 0 to 1, which is a measure of the probability that the jet is an EJ. Tracks are associated with

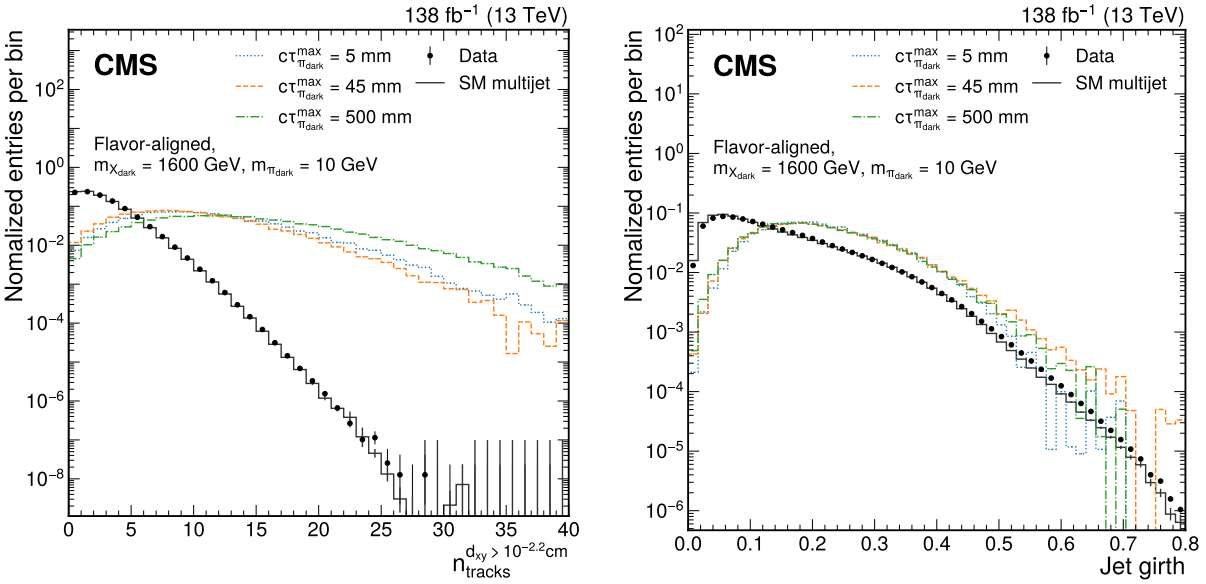

Figure 3: Distributions of the jet variables used for the model-agnostic EJ tagging targeting flavor-aligned dark sector models for jets obtained in data (points), SM multijet simulation (gray line), and simulated signal jets (colored lines). The distribution of the number of tracks with $d_{xy} > 10^{-2.2}$ cm (jet girth) is shown on the left (right). The sums of the entries are normalized to unity.

a jet using $R_{\text{max}} = 0.8$. To maximize the available information for the ML training, the tracks are not required to satisfy a d_z^{max} requirement. Each network is trained on all jets originating from a dark quark in the signal models of interest, and an equal number of jets taken from SM QCD simulation as the background sample.

The $\Delta\eta$ and $\Delta\phi$ between each track and its associated jet are used as the track coordinate variables in the jet space. Each track in the jet is represented by a 5-feature vector containing:

- $\Delta R(\text{track}, \text{jet})$, as particles in EJs tend to have a wider angular separation than in the SM jets because of the heaviness of the dark mesons.
- $\ln(p_{\text{T}}^{\text{track}}/1\,\text{GeV})$, $\ln(p_{\text{T}}^{\text{track}}/\sum_i p_{\text{T}}^i)$, as the combination of the dark shower and the decay of the mesons back to the SM sector causes the p_{T} of tracks to be smaller on average for EJs than for SM jets.
- $T(d_{xy})$, $T(d_z)$. The transformation function $T(x)$ is applied to the track displacement variables, to reduce the range of values input to the GNN while preserving the variables' sign and continuity. It is defined as:

$$T(x) = \text{sign}(x) \ln\left(\left|\frac{x}{1\,\text{cm}}\right| + 1\right).$$

  This transformation was found to give comparable or better performance than a standard scaling.

The impact parameter d_{xy} is the most influential feature. Figure 4 shows the output score distributions for signal and background, demonstrating good separation. The signal distributions are similar despite the wide range of dark meson $c\tau$ values.

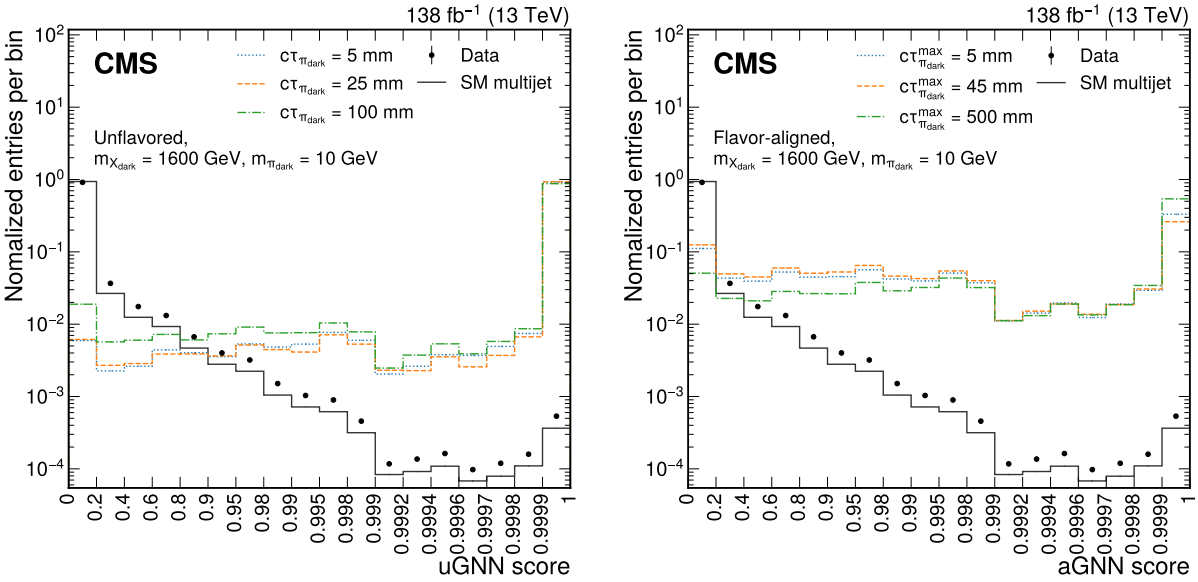

Figure 4: Distributions of the output score of the uGNN (left) and aGNN (right) for the data (points with error bars), SM multijet simulation (dark gray line), and signal simulation (colored lines). The signal distributions in the left (right) plot are generated from the unflavored (flavor-aligned) model. Bins are chosen to correspond to the jet selection criteria defined in Table 5. The sums of the entries are normalized to unity.

5.3 Determining the EJ tagging and event selection criteria

An optimization procedure is performed for each signal model to determine the best threshold on the event H_T, jet p_T, and the EJ tagging variables by maximizing σ_{opt}, defined as:

$$\sigma_{opt} = \frac{S}{\sqrt{S + B + \beta^2 B^2}}, \tag{3}$$

where S (B) is the number of simulated signal (background multijet) events passing the selection thresholds and β is the estimated relative systematic uncertainty in the background, taken to be 10%. To reduce the number of sets of selection criteria, similar selection sets are grouped, and a representative set that gives at least 90% of the original best significance value is used for all the models in the group. Additional selection sets with higher background selection efficiencies are used to validate the background estimation calculations. Their selection criteria are detailed in Section 5.4.

The selection criteria used for EJ tagging are shown in Tables 3–5, and those for the event selection in Table 6. For the unflavored model, at $c\tau_{\pi_{dark}} = 45$ mm, the model-agnostic taggers yield a maximum signal selection efficiency of ≈40%, while the ML-based taggers yield a maximum signal selection efficiency of ≈60%. The signal selection efficiency of the model-agnostic taggers drops to a few percent for very short-lived (≈1 mm) dark pions, and the efficiency of both taggers drops to a few percent for very long-lived (≈1000 mm) dark pions. For the flavor-aligned model, at $c\tau^{max}_{\pi_{dark}} = 45$ mm, the model-agnostic taggers yield a maximum signal selection efficiency of ≈25%, while the ML-based taggers yield a maximum signal selection efficiency of ≈40%. This efficiency remains fairly stable along the full maximum lifetime range for both taggers.

Table 3: Emerging jet selection criteria for the model-agnostic analysis designed for the unflavored scenario. The validation regions are discussed in Section 5.4. The symbols in parentheses indicate a minimum (>) or maximum (<) requirement.

Tag name	d_z [cm] (<)	$\left\langle d_{xy} \right\rangle$ [cm] (>)	D_N (<)	α_{3D} (<)
u-tag 1	0.5	$10^{-1.6}$	4.0	0.25
u-tag 2	1.0	$10^{-1.4}$	8.0	0.25
u-tag 3	5.0	$10^{-1.2}$	8.0	0.25
u-tag 4	5.0	$10^{-1.2}$	12.0	0.15
u-tag 5	5.0	$10^{-1.0}$	12.0	0.15
validation u-tag	0.5	$10^{-1.6}$	4.0	0.40

Table 4: Emerging jet selection criteria for the model-agnostic analysis designed for the flavor-aligned scenario. The validation tag is described in Section 5.4. The symbols in parentheses indicate a minimum (>) or maximum (<) requirement.

Tag name	d_z [cm] (<)	d_{xy}^{min} [cm]	$n_{\text{track}}^{d_{xy}>d_{xy}^{\text{min}}}$ (>)	Jet girth (>)
a-tag 1	0.5	$10^{-2.2}$	12	0.05
a-tag 2	0.5	$10^{-2.2}$	12	0.1
a-tag 3	0.5	$10^{-2.3}$	14	0.0
a-tag 4	0.5	$10^{-2.4}$	14	0.1
validation a-tag	0.5	$10^{-2.4}$	12	0.0

5.4 Background estimation

The signal region (SR) for this analysis is constructed from events with two or more tagged EJs. The main source of background for this analysis is the production of four SM jets, where two or more of these jets are misidentified as EJs. We estimate the number of SM events passing the selection criteria in the SR by constructing a control region (CR) with identical event and jet kinematic requirements, but where exactly one jet is tagged as an EJ. We estimate the fraction of signal events in the CR to be no more than 10^{-5}. The probability of an SM jet being misidentified as an EJ (mistag rate) is heavily dependent on the underlying jet flavor, as SM jets containing b hadrons also have displaced tracks. We therefore estimate the misidentification probability $\epsilon(f, p_{\text{T}})$ as a function of the underlying jet flavor f, where f is b for b jets and q for other jet flavors, and the jet p_{T}.

Table 5: The GNN score range used to identify a jet as an EJ. The uGNN (aGNN) tag indicates that the tagger uses the output score of the GNN trained on the unflavored (flavor-aligned) simulated signal samples. The validation tags are described in Section 5.4.

Tag name	Score min.	Score max.
uGNN tag 1	0.9997	1
uGNN tag 2	0.9998	1
uGNN tag 3	0.9996	1
uGNN validation tag	0.998	0.9995
aGNN tag 1	0.9953	1
aGNN tag 2	0.9993	1
aGNN tag 3	0.9983	1
aGNN validation tag	0.99	0.995

Table 6: Event selection criteria used for the analysis. The validation selection criteria are described in Section 5.4.

Selection set	H_T [GeV]	Jet p_T [GeV] (>)				EJ tagger
u-set 1	>1600	275	250	250	150	u-tag 1
u-set 2	>1600	200	200	150	150	u-tag 2
u-set 3	>1600	200	150	100	100	u-tag 3
u-set 4	>1500	200	150	100	100	u-tag 4
u-set 5	>1200	200	150	100	100	u-tag 5
u-set validation	1000–1200	100	100	100	100	validation u-tag
a-set 1	>1500	200	150	100	100	a-tag 1
a-set 2	>1800	250	250	200	200	a-tag 2
a-set 3	>1200	275	250	250	200	a-tag 2
a-set 4	>1500	275	250	250	100	a-tag 3
a-set 5	>1800	200	150	100	100	a-tag 4
a-set validation	1000–1200	100	100	100	100	validation a-tag
uGNN set 1	>1350	170	120	120	100	uGNN tag 1
uGNN set 2	>1750	300	260	250	250	uGNN tag 2
uGNN set 3	>1800	240	180	180	100	uGNN tag 3
uGNN validation	>1000	100	100	100	100	uGNN validation tag
aGNN set 1	>1300	200	140	120	100	aGNN tag 1
aGNN set 2	>1650	300	250	200	200	aGNN tag 2
aGNN set 3	>1400	270	220	220	120	aGNN tag 3
aGNN validation	>1000	100	100	100	100	aGNN validation tag

Assuming that the probability of a jet being misidentified as an EJ is independent of the multiplicity and properties of other jets in the event, the number of background events in the SR is estimated using counts in the CR and the mistag rate according to the following formula:

$$N_{\mathrm{SR}} = \sum_{\text{events} \in \mathrm{CR}} \frac{\frac{1}{2!}\left(\sum_i \epsilon_i \prod_{j\neq i}(1-\epsilon_j)\right) + \frac{1}{3!}\left(\sum_{i\neq j} \epsilon_i \epsilon_j \prod_{k\neq i,j}(1-\epsilon_k)\right) + \frac{1}{4!}\left(\sum_{i\neq j\neq k} \epsilon_i \epsilon_j \epsilon_k\right)}{\prod_i (1-\epsilon_i)}, \tag{4}$$

where ϵ_i is an abbreviation of $\epsilon(f_i, p_{\mathrm{T}}^i)$, the estimated mistag rate of jet i in each event. The jet indices in the summations and products run over all jets that are not EJ tagged. Because the underlying flavor of each jet is difficult to determine, we approximate ϵ_i in Eq.(4) using a flavor-fraction-averaged misidentification rate $\epsilon^{\mathrm{avg}}(p_{\mathrm{T}})$ and the estimated b jet fraction $F_{\mathrm{b}}^{\mathrm{CR}}$ of all non EJ-tagged jets in the CR:

$$\epsilon^{\mathrm{avg}}(p_{\mathrm{T}}) = F_{\mathrm{b}}^{\mathrm{CR}} \epsilon(\mathrm{b}, p_{\mathrm{T}}) + \left(1 - F_{\mathrm{b}}^{\mathrm{CR}}\right) \epsilon(\mathrm{q}, p_{\mathrm{T}}). \tag{5}$$

The value of $F_{\mathrm{b}}^{\mathrm{CR}}$ is estimated by fitting the CMS DEEPJET discriminator [42] spectrum of the non EJ-tagged jets in the CR to two template distributions obtained from SM multijet MC events. One template contains the discriminator value for jets identified using generator-level information as containing a b quark, and the complement template is used for the other jets. The template distributions are varied within the measured uncertainties [43, 44]. The fit is performed for each of the selection criteria listed in Table 6. Figure 5 gives an example of the fit performance for the "u-set validation" selection criteria, defined in Table 6.

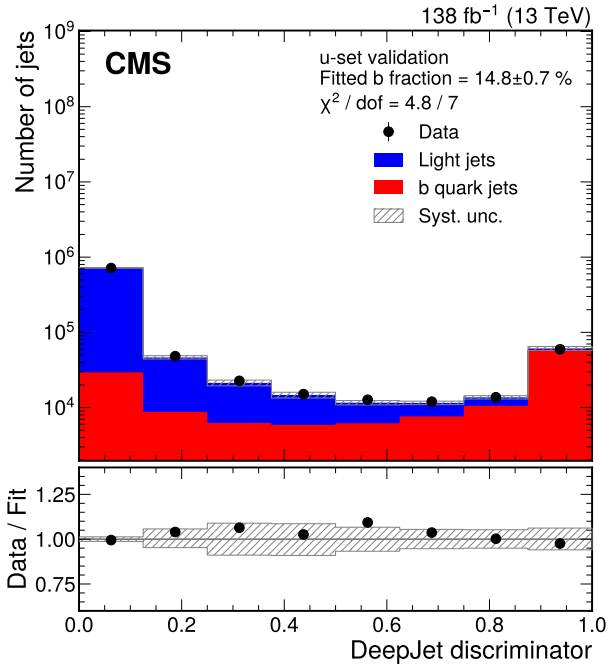

Figure 5: Template fit of the DEEPJET discriminator used to determine the b jet fraction of the non-EJ tagged jets for data events that pass the "u-set validation" selection criteria, except with the requirement on the number of EJ-tagged jets changed from 2 to 1. The lower panel shows the ratio of the number of jets in the data compared to the sum of the fitted template distributions.

The evaluation of the mistag rate is performed in a signal-free region (FR) that consists of events passing a high-p_T photon trigger and containing an isolated photon in the ECAL barrel with $p_T > 200\,\text{GeV}$. The FR events are required to have either one or two jets passing the jet selection criteria described in Section 5.1. To obtain the misidentification probability for different jet flavors, we further divide the FR into a b-enriched region (ER) and a b-depleted region (DR) by imposing b tagging requirements on an additional jet with $p_T > 50\,\text{GeV}$ and $|\eta| < 2.4$ that passes a set of noise-rejection criteria [49]. As a significant fraction of heavy-flavored jets originate from gluon splitting in this event sample, b tagging requirements on this extra jet will change the b jet fraction of the selected jets. Events are classified as ER if the additional jet passes DEEPJET b tagging at the medium working point, and are classified as DR if the additional jet fails DEEPJET b tagging at the loose working point. Assuming that the ER and DR have the same mistag probabilities for the selected jets, and the only difference between these regions is the overall b jet fraction, the misidentification rate for all the selected jets in a specific region XR, $\epsilon^{\text{XR}}(p_T)$, can be expressed as a linear combination of $\epsilon(\text{b}, p_T)$ and $\epsilon(\text{q}, p_T)$:

$$\begin{aligned}\epsilon^{\text{ER}}(p_T) &= F_{\text{b}}^{\text{ER}}(p_T)\epsilon(\text{b}, p_T) + \left(1 - F_{\text{b}}^{\text{ER}}(p_T)\right)\epsilon(\text{q}, p_T),\\ \epsilon^{\text{DR}}(p_T) &= F_{\text{b}}^{\text{DR}}(p_T)\epsilon(\text{b}, p_T) + \left(1 - F_{\text{b}}^{\text{DR}}(p_T)\right)\epsilon(\text{q}, p_T),\end{aligned} \tag{6}$$

where $F_{\text{b}}^{\text{XR}}(p_T)$ is the estimated b jet fraction of region XR in bins of jet p_T. The b jet fraction is obtained by fitting the DEEPJET b discriminator distribution to templates obtained using jets from a simulated γ+jets sample. On average, the selected jets in the ER and DR have b jet fractions of 15% and 4%, respectively. The linear relation in Eq. (6) can then be inverted to obtain the mistag rates for different underlying jet flavors $\epsilon(f, p_T)$, which is used in Eq. (5) to estimate the misidentification rate of jets in the CR. Figure 6 gives examples of the estimated

EJ tagger misidentification probabilities for "u-tag 1" and "uGNN tag 1" taggers, defined in Tables 3 and 5.

Because the Phase 1 upgrade of the pixel detector [23] improved the track reconstruction performance, the evaluation of the expected background is performed separately for the pixel Phase 0 geometry (2016) and Phase 1 geometry (2017–2018).

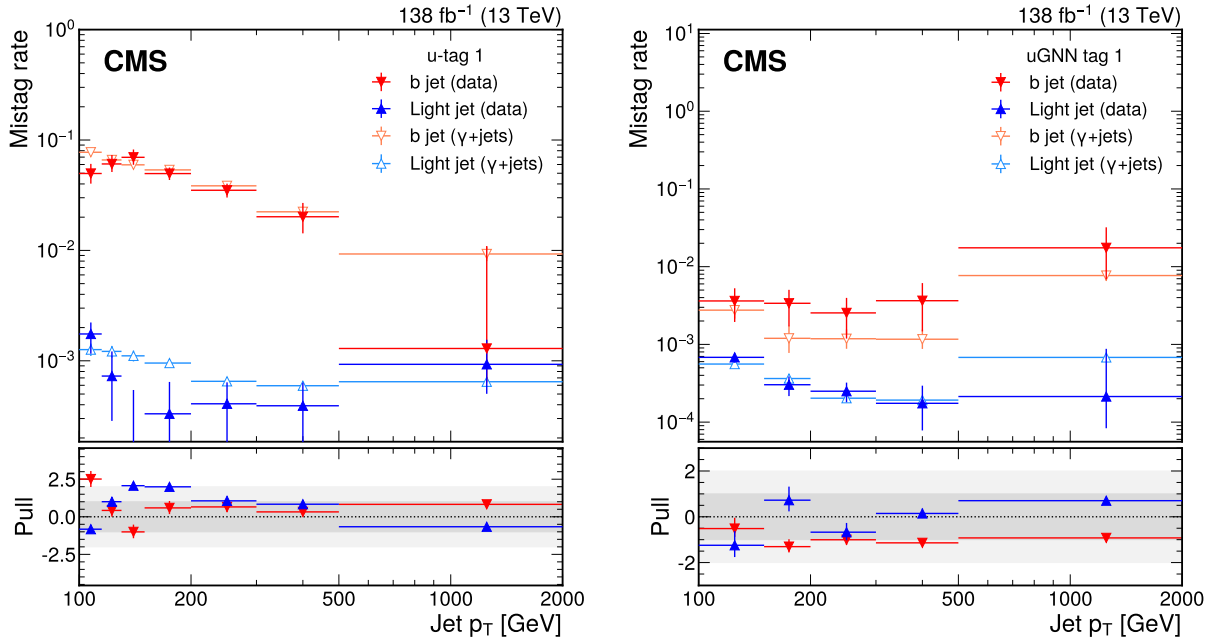

Figure 6: The EJ tagger misidentification probability for b quark jets (red, orange) and light jets (light blue, dark blue) as a function of jet p_T for the model-agnostic tagger "u-tag 1" (left) and the ML-based tagger "uGNN tag 1" (right), as defined in Tables 3 and 5, evaluated using data (red, dark blue) and generator-level flavor information from simulated samples (orange, light blue) in events containing a high-p_T photon. The lower panel shows the pull, defined as the difference between the mistag rate calculated in simulation and mistag rate measured in data divided by the uncertainty measured in data.

To validate the background estimation, closure tests are performed in validation regions (VRs) that use selection criteria that are orthogonal to the SRs. The VRs are defined using signal-like selection criteria that require at least two jets passing a validation EJ tagger. The observed number of events in the VR is compared to the number predicted using our background estimation technique. For the model-agnostic EJ tagging VR, the H_T requirement of the validation event selection is inverted to ensure orthogonality with the SRs and small signal contamination. The EJ identification requirements for the validation EJ tagger are based on the u-tag 1 and a-tag 1 requirements for unflavored and flavor-aligned models, respectively, with one jet-variable selection requirement relaxed to further reduce the effect of any small signal contamination. The VR for the ML-based EJ tagging uses a validation tagger that selects jets with GNN scores in a region disjoint from the SRs. To further increase the number of events that pass the ML-based VR, we relax the H_T and jet p_T requirements. The full list of the selection criteria used for the VRs is given in Tables 3–6. The signal contamination in these VRs is less than 1% for all surveyed signal models.

The number of events passing the VR selection criteria with at least two jets passing the validation jet tag, as well as the predicted number using the estimation described in Eq. (4), is given in Table 7. No significant deviation between the observed and the estimation results is observed,

indicating that the background estimation calculation is robust.

Table 7: The observed yield of events in data satisfying the validation selection criteria with at least two jets passing the corresponding validation tag, and the estimation based on the misidentification rate calculated using validation events with exactly one jet passing the validation tagger scaled by the factor given in Eq. (4). The statistical and systematic uncertainties are reported for the estimated yields.

Selection set	Estimation $\pm$ stat. $\pm$ syst.	Observed yield
u-set validation	$1220 \; ^{+\,80}_{-\,80} \pm 210$	1484
a-set validation	$77 \; ^{+\,4}_{-\,4} \pm 15$	118
uGNN validation	$29.3 \; ^{+\,7.0}_{-\,3.4} \pm 8.2$	21
aGNN validation	$29.1 \; ^{+\,6.1}_{-\,2.6} \pm 5.2$	37

6 Systematic uncertainties

6.1 Background uncertainties

The main sources of systematic uncertainty in this search arise from the background estimation method based on control samples in data. The kinematic differences between the SM jets in the CR photon-triggered data used for the misidentification rate calculation and the SM jets in the H_{T}-triggered data used in the SR may lead to slightly different misidentification rates. We estimate the corresponding uncertainties by applying the background prediction method in Eq. (4) to simulated SM multijets events, using either the mistag rate from the SM multijet simulation or from the γ+jets simulation. The uncertainty is taken as the difference in the background predictions obtained with the two mistag rates. There is also an uncertainty in the flavor composition used in the misidentification rate estimations. This uncertainty is estimated from simulated background events by comparing the flavor-decomposition estimate described in Section 5.4 with one derived from generator-level flavor information. Finally, there is the uncertainty associated with the choice of variables used to parameterize the mistag rate. This uncertainty is estimated by comparing the estimation results when parameterizing the mistag rate as a function of jet p_{T} versus track multiplicity, as these are the variables for which the mistag rate shows the most significant dependence. The selection variables $\left\langle d_{xy} \right\rangle$ and α_{3D} used in the model-agnostic taggers have an intrinsic dependence on the track multiplicity, making the mistag rate parameterization uncertainty more pronounced in the model-agnostic method. These three uncertainty sources are considered to be uncorrelated and summed in quadrature. The resulting uncertainties are given in Tables 7 and 9.

6.2 Signal uncertainties

Various sources of uncertainty affecting the signal yields are also considered. The integrated luminosity uncertainties for the 2016, 2017, and 2018 data-taking periods are 1.2, 2.3, and 2.5%, respectively [52–54]. The trigger efficiency is slightly different in data and simulation. A correction factor compensates for this difference, and its statistical uncertainty is propagated to an uncertainty in the signal acceptance. The evaluation of jet energy correction uncertainties is performed as a function of jet p_{T} and η, propagated to all jet-related kinematic variables, and then to an uncertainty in the signal acceptance. Uncertainty sources are treated as fully

correlated across the years for the jet energy scale (JES), and uncorrelated for the jet energy resolution (JER). While the pileup distribution in the simulation is reweighted to match the data, there is a 4.6% uncertainty in the total inelastic cross section [55], which is treated as fully correlated across the years. The impact parameter distribution is slightly broader in the data CRs than in simulation. A smearing function that corrects this is applied to tracks in the simulated samples, and the resulting changes to the signal acceptances are used to estimate the modeling uncertainty. The corrected values are also used to recompute the GNN score. The uncertainty in the acceptance from the uncertainties in the PDFs is evaluated by reweighting events with different PDF variations [34, 56]. As reconstruction efficiency differences between data and simulation for displaced tracks are difficult to evaluate, we varied the reconstruction efficiency for tracks with $d_{xy} > 4\,\text{cm}$ (approximately the distance to the second layer of the pixel detector) by 10% and found an ≈1% overall change in signal acceptance. As the measured difference in reconstruction efficiency in data and MC is expected to be much smaller (on the order of 1–2% [57]), no uncertainty is assigned. The uncertainty from the factorization scale (μ_F) and renormalization scale (μ_R) choices is estimated by independently varying μ_F and μ_R by factors of 2 and 0.5 [58, 59]. A summary of the estimated uncertainties for the various signal model acceptances is given in Table 8.

Table 8: Mean and standard deviation (std.) of the relative uncertainty calculated on the unflavored and flavor-aligned samples, by source, in percent.

	Model-agnostic taggers				ML-based taggers			
Uncertainty source	Unflavored		Flavor-aligned		Unflavored		Flavor-aligned	
	mean	std.	mean	std.	mean	std.	mean	std.
Integrated luminosity	1.8	0.6	1.8	0.6	1.8	0.6	1.8	0.6
Trigger efficiency	0.3	0.1	0.3	0.1	0.3	0.1	0.3	0.1
JES	1.0	1.3	0.8	0.7	1.3	0.9	0.7	0.4
JER	0.3	0.4	0.3	0.3	0.2	0.3	0.2	0.1
Pileup reweighting	1.6	1.4	1.4	1.2	0.9	0.8	1.0	0.9
Track modeling in sim.	0.2	0.3	1.4	1.8	0.3	0.8	0.5	0.6
PDF	<0.1	<0.1	<0.1	<0.1	<0.1	< 0.1	<0.1	<0.1
μ_F, μ_R	<0.1	<0.1	<0.1	<0.1	<0.1	<0.1	<0.1	<0.1

7 Results

After the full event selection, the observed and expected event yields corresponding to each selection set are shown in Table 9. No statistically significant deviation from the SM background prediction is observed. The observation is used to set upper limits on the various signal parameter models considered using the CL_s criterion [60, 61]. The test statistic is defined as the likelihood ratio employed in Higgs boson analyses in ATLAS and CMS, as elaborated in Ref. [62]. Upper limits at the 95% confidence level (CL) on the production cross section in the 2-dimensional plane defined by the signal parameters are shown in Figs. 7 ($m_{\pi_\text{dark}} = 10\,\text{GeV}$) and 8 ($m_{\pi_\text{dark}} = 20\,\text{GeV}$) for both the unflavored and the flavor-aligned scenarios, and in Fig. 9 ($m_{\pi_\text{dark}} = 6\,\text{GeV}$) for the flavor-aligned scenario. These excluded cross sections are compared to the theoretical prediction to derive the exclusion regions shown as red and black curves for the expected and observed 95% CL limit, respectively. The red curves also have an associated red band to indicate the 68% CL variation on the expected exclusion limit.

In the unflavored coupling model, the key tagging variable for the model-agnostic method is the mean d_{xy} of the associated tracks in the jet. In the case where the dark pion lifetime is too

Table 9: The estimated number of events from the background prediction based on control samples in data and the observed event yields. Statistical and systematic uncertainties in the estimated background are provided.

Selection set	Estimation $\pm$ stat. $\pm$ syst.	Observed yield
u-set 1	$56 \; ^{+\,9}_{-\,5} \pm 20$	67
u-set 2	$20.0 \; ^{+\,4.3}_{-\,2.5} \pm 7.0$	21
u-set 3	$22.9 \; ^{+\,7.3}_{-\,2.1} \pm 4.9$	24
u-set 4	$7.9 \; ^{+\,2.0}_{-\,1.6} \pm 2.2$	10
u-set 5	$11.3 \; ^{+\,2.7}_{-\,1.9} \pm 2.0$	13
a-set 1	$8.8 \; ^{+\,2.4}_{-\,1.0} \pm 2.0$	16
a-set 2	$1.67 \; ^{+\,0.49}_{-\,0.23} \pm 0.38$	3
a-set 3	$1.97 \; ^{+\,0.47}_{-\,0.22} \pm 0.37$	2
a-set 4	$2.30 \; ^{+\,0.81}_{-\,0.30} \pm 0.39$	3
a-set 5	$10.2 \; ^{+\,2.3}_{-\,1.1} \pm 3.4$	16
uGNN set 1	$15.6 \; ^{+\,5.4}_{-\,1.9} \pm 3.8$	18
uGNN set 2	$0.73 \; ^{+\,0.44}_{-\,0.16} \pm 0.27$	0
uGNN set 3	$7.6 \; ^{+\,3.5}_{-\,1.3} \pm 2.3$	9
aGNN set 1	$45 \; ^{+\,18}_{-\,8} \pm 16$	59
aGNN set 2	$0.30 \; ^{+\,0.23}_{-\,0.07} \pm 0.18$	1
aGNN set 3	$3.8 \; ^{+\,2.2}_{-\,0.7} \pm 2.0$	5

short, the displaced tracks from the dark pion decay products will be very similar to prompt SM tracks. In the opposite case, where the dark pion lifetime is very large, the dark pions increasingly decay outside the tracker. Thus, this search method is less sensitive to these two cases, giving reduced performance, as shown in the upper-left plots of Figs. 7 and 8. In contrast, the GNN method performs well even at low dark pion lifetimes, as the signal acceptance remains high. However, signal sensitivity is still limited for long dark pion lifetimes, as shown in the upper-right plots of Figs. 7 and 8.

In the flavor-aligned scenario, the differentiating power for the model-agnostic method comes mainly from the multiplicity of associated tracks with large displacements. Unlike d_{xy}, the multiplicity distribution is more uniform for different dark pion lifetimes (as we only consider $c\tau^{\text{max}}_{\pi_{\text{dark}}}$ above the typical b hadron lifetime) leading to less dependence on $c\tau^{\text{max}}_{\pi_{\text{dark}}}$ as seen in the lower-left plots of Figs. 7 and 8. Similarly, the GNN is also not sensitive to changes in lifetime, resulting in a stable signal acceptance across the $c\tau^{\text{max}}_{\pi_{\text{dark}}}$ range. In the flavor-aligned models where $m_{\pi_{\text{dark}}} = 6\,\text{GeV}$, the dark pions decay predominantly to light SM quarks because of mass constraints, resulting in fewer displaced tracks in the events. This reduces the selection efficiencies for these signal models, leading to the model-agnostic method having less sensitivity compared to models with larger $m_{\pi_{\text{dark}}}$, as shown in Fig. 9.

The ML-based EJ tagging methods yield more stringent limits on the surveyed models. In the

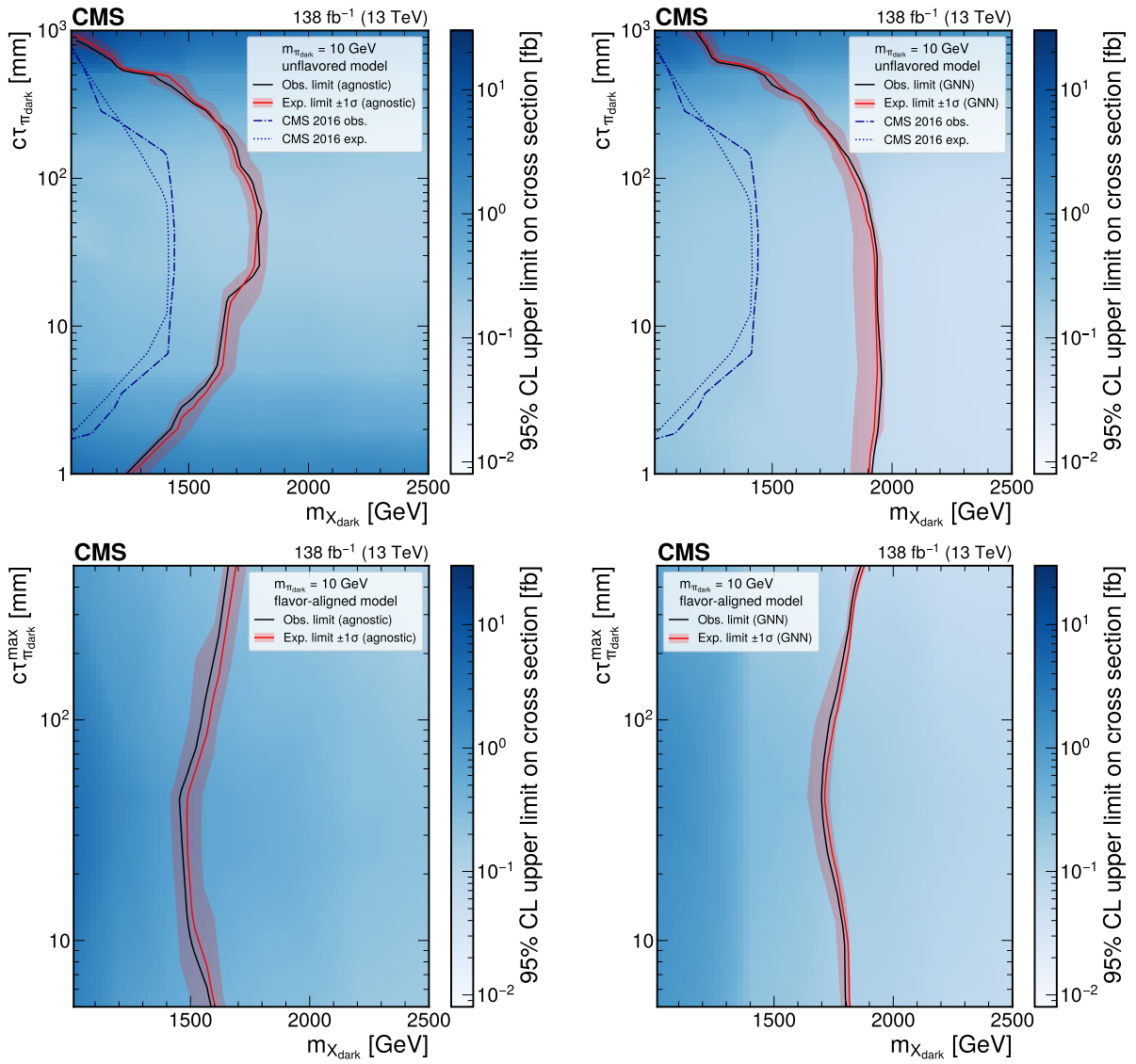

Figure 7: The 95% CL upper limits on the production cross section for various signal models in the unflavored scenario (upper plots) and the flavor-aligned scenario (lower plots) with $m_{\pi_{\text{dark}}} = 10\,\text{GeV}$ using the model-agnostic (GNN) EJ tagging method, on the left (right). The red curve is the expected exclusion limit, with the band representing its 68% CL variation. The black curve is the observed limit. The dark blue dotted curves in the upper plots are the expected and observed limits previously obtained by CMS [20].

unflavored model, X_{dark} masses up to 1900 and 1950 GeV are excluded at 95% CL for $m_{\pi_{\text{dark}}}$ of 10 and 20 GeV, respectively, closely matching the expected limits. For the flavor-aligned models, the X_{dark} mass exclusion at 95% CL increases to 1950, 1850, and 1900 GeV for $m_{\pi_{\text{dark}}}$ of 6, 10, and 20 GeV, respectively, again matching well the expected limits. Relative to the model-agnostic tagger, the greatest increase in sensitivity is for the unflavored signal models with short lifetimes, where the dark showers generate nearly prompt tracks that are difficult to tag using simple requirements on the track displacement variables.

The GNN-based limits for the flavor-aligned models that utilize the aGNN set 2 selection have a narrow expected band, as shown in the lower right plots of Figs. 7–8 and the right plot of Fig. 9. For that selection set, 0.3 background events are predicted, which implies that the most frequent

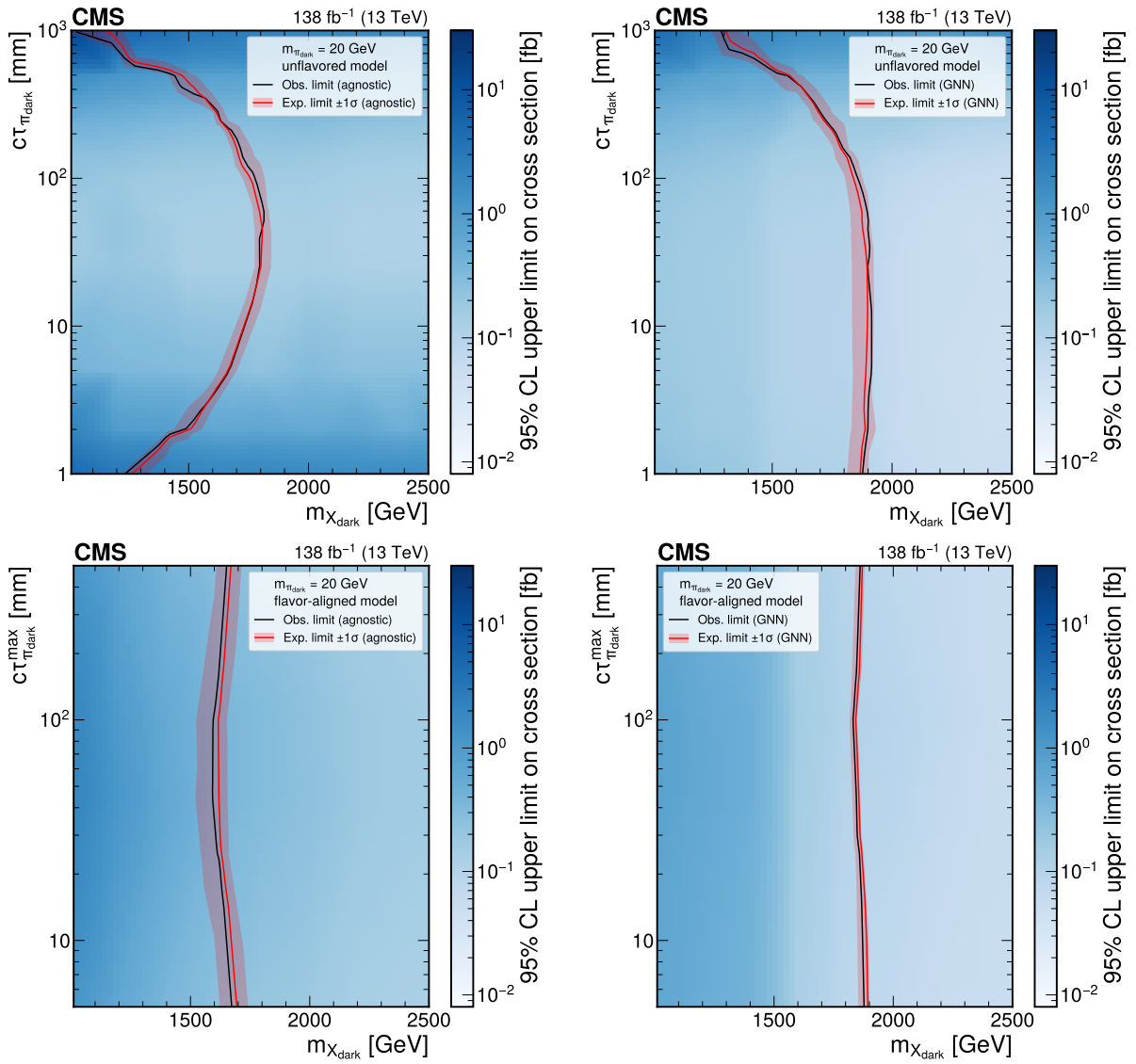

Figure 8: The 95% CL upper limits on the production cross section for various signal models in the unflavored scenario (upper plots) and the flavor-aligned scenario (lower plots) with $m_{\pi_{\mathrm{dark}}} = 20\,\mathrm{GeV}$ using the model-agnostic (GNN) EJ tagging method, on the left (right). The red curve is the expected exclusion limit, with the band representing its 68% CL variation. The black curve is the observed limit.

observation will be exactly zero events if the background-only hypothesis is correct. Because the likelihood function is constructed from Poisson probabilities, this leads to the background-only test statistic distribution exhibiting discrete, narrow peaks. With a free-floating signal strength, the test statistic distribution for the signal plus background hypothesis shares similar features. As a result, only a small change in the signal strength is required to obtain a $\mathrm{CL_s}$ value of 0.05 when going from 95 to 68% CL to the expected median of the background expectation. The resulting expected limit bands in this region are narrow and asymmetrical.

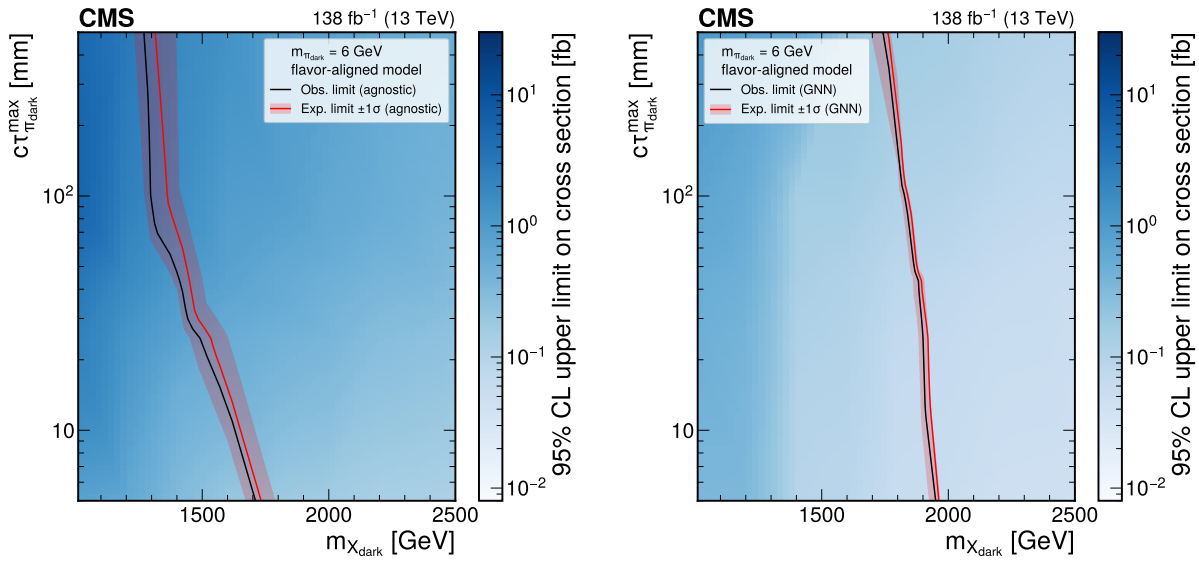

Figure 9: The 95% CL upper limits on the production cross section for various signal models in the flavor-aligned scenario with $m_{\pi_{\text{dark}}} = 6\,\text{GeV}$ using the model-agnostic (GNN) EJ tagging method, on the left (right). The red curve is the expected exclusion limit, with the band representing its 68% CL variation. The black curve is the observed limit.

8 Summary

A search for emerging jet signatures arising from a strongly interacting dark sector produced in proton-proton collisions has been presented, using data corresponding to an integrated luminosity of $138\,\text{fb}^{-1}$ at $\sqrt{s} = 13\,\text{TeV}$. The signal model contains a family of dark quarks that couple to the standard model (SM) quarks via a scalar mediator X_{dark}. Dark pions (π_{dark}) with a significant lifetime ($c\tau_{\pi_{\text{dark}}}$) are produced by the hadronization of the dark quarks; these then decay to SM particles at vertices displaced from the proton-proton interaction point. As the scalar mediator is assumed to be produced in pairs, and each decays to an SM quark and a dark quark, the signature of this process is two SM jets plus two jets of particles with constituents emerging from displaced vertices.

Both unflavored and flavor-aligned couplings between the SM quarks and the dark quarks are examined in the search. Events are selected using either a traditional cut-based approach or a graph neural network to identify emerging jets, in combination with other event-level selection criteria. The overall selection requirements are optimized for each coupling scenario and for different combinations of the mediator particle mass, dark pion mass, and dark pion lifetime. No excess of events beyond the SM expectations is found, and the observed 95% confidence level exclusion limits agree with the expected limits. For the unflavored model, dark mediator masses $m_{X_{\text{dark}}} < 1950\,\text{GeV}$ are excluded for $c\tau_{\pi_{\text{dark}}} \approx 100\,\text{mm}$ and $m_{\pi_{\text{dark}}} = 10\,\text{GeV}$, while the flavor-aligned model result excludes $m_{X_{\text{dark}}} < 1850\,\text{GeV}$ at $c\tau^{\text{max}}_{\pi_{\text{dark}}} \approx 500\,\text{mm}$ for $m_{\pi_{\text{dark}}} = 10\,\text{GeV}$. This result surpasses the previous search for emerging jets in the unflavored scenario, increasing the experimental limit of the dark mediator particle by ≈500 GeV to set the most stringent limits to date, and provides the first direct exclusion of the flavor-aligned scenario.

Acknowledgments

We congratulate our colleagues in the CERN accelerator departments for the excellent performance of the LHC and thank the technical and administrative staffs at CERN and at other CMS institutes for their contributions to the success of the CMS effort. In addition, we gratefully acknowledge the computing centers and personnel of the Worldwide LHC Computing Grid and other centers for delivering so effectively the computing infrastructure essential to our analyses. Finally, we acknowledge the enduring support for the construction and operation of the LHC, the CMS detector, and the supporting computing infrastructure provided by the following funding agencies: SC (Armenia), BMBWF and FWF (Austria); FNRS and FWO (Belgium); CNPq, CAPES, FAPERJ, FAPERGS, and FAPESP (Brazil); MES and BNSF (Bulgaria); CERN; CAS, MoST, and NSFC (China); MINCIENCIAS (Colombia); MSES and CSF (Croatia); RIF (Cyprus); SENESCYT (Ecuador); ERC PRG, RVTT3 and MoER TK202 (Estonia); Academy of Finland, MEC, and HIP (Finland); CEA and CNRS/IN2P3 (France); SRNSF (Georgia); BMBF, DFG, and HGF (Germany); GSRI (Greece); NKFIH (Hungary); DAE and DST (India); IPM (Iran); SFI (Ireland); INFN (Italy); MSIP and NRF (Republic of Korea); MES (Latvia); LMTLT (Lithuania); MOE and UM (Malaysia); BUAP, CINVESTAV, CONACYT, LNS, SEP, and UASLP-FAI (Mexico); MOS (Montenegro); MBIE (New Zealand); PAEC (Pakistan); MES and NSC (Poland); FCT (Portugal); MESTD (Serbia); MCIN/AEI and PCTI (Spain); MOSTR (Sri Lanka); Swiss Funding Agencies (Switzerland); MST (Taipei); MHESI and NSTDA (Thailand); TUBITAK and TENMAK (Turkey); NASU (Ukraine); STFC (United Kingdom); DOE and NSF (USA).

Individuals have received support from the Marie-Curie program and the European Research Council and Horizon 2020 Grant, contract Nos. 675440, 724704, 752730, 758316, 765710, 824093, 101115353, and COST Action CA16108 (European Union); the Leventis Foundation; the Alfred P. Sloan Foundation; the Alexander von Humboldt Foundation; the Science Committee, project no. 22rl-037 (Armenia); the Belgian Federal Science Policy Office; the Fonds pour la Formation à la Recherche dans l'Industrie et dans l'Agriculture (FRIA-Belgium); the Agentschap voor Innovatie door Wetenschap en Technologie (IWT-Belgium); the F.R.S.-FNRS and FWO (Belgium) under the "Excellence of Science – EOS" – be.h project n. 30820817; the Beijing Municipal Science & Technology Commission, No. Z191100007219010 and Fundamental Research Funds for the Central Universities (China); the Ministry of Education, Youth and Sports (MEYS) of the Czech Republic; the Shota Rustaveli National Science Foundation, grant FR-22-985 (Georgia); the Deutsche Forschungsgemeinschaft (DFG), under Germany's Excellence Strategy – EXC 2121 "Quantum Universe" – 390833306, and under project number 400140256 - GRK2497; the Hellenic Foundation for Research and Innovation (HFRI), Project Number 2288 (Greece); the Hungarian Academy of Sciences, the New National Excellence Program - ÚNKP, the NKFIH research grants K 124845, K 124850, K 128713, K 128786, K 129058, K 131991, K 133046, K 138136, K 143460, K 143477, 2020-2.2.1-ED-2021-00181, and TKP2021-NKTA-64 (Hungary); the Council of Science and Industrial Research, India; ICSC – National Research Center for High Performance Computing, Big Data and Quantum Computing, funded by the EU NexGeneration program (Italy); the Latvian Council of Science; the Ministry of Education and Science, project no. 2022/WK/14, and the National Science Center, contracts Opus 2021/41/B/ST2/01369 and 2021/43/B/ST2/01552 (Poland); the Fundação para a Ciência e a Tecnologia, grant CEECIND/01334/2018 (Portugal); the National Priorities Research Program by Qatar National Research Fund; MCIN/AEI/10.13039/501100011033, ERDF "a way of making Europe", and the Programa Estatal de Fomento de la Investigación Científica y Técnica de Excelencia María de Maeztu, grant MDM-2017-0765 and Programa Severo Ochoa del Principado de Asturias (Spain); the Chulalongkorn Academic into Its 2nd Century Project Advance-

ment Project, and the National Science, Research and Innovation Fund via the Program Management Unit for Human Resources & Institutional Development, Research and Innovation, grant B37G660013 (Thailand); the Kavli Foundation; the Nvidia Corporation; the SuperMicro Corporation; the Welch Foundation, contract C-1845; and the Weston Havens Foundation (USA).

References

[1] V. C. Rubin, N. Thonnard, and W. K. Ford, Jr., "Rotational properties of 21 SC galaxies with a large range of luminosities and radii, from NGC 4605 (R = 4 kpc) to UGC 2885 (R = 122 kpc)", *Astrophys. J.* **238** (1980) 471, doi:10.1086/158003.

[2] M. Persic, P. Salucci, and F. Stel, "The universal rotation curve of spiral galaxies: I. The dark matter connection", *Mon. Not. Roy. Astron. Soc.* **281** (1996) 27, doi:10.1093/mnras/278.1.27, arXiv:astro-ph/9506004.

[3] D. Clowe et al., "A direct empirical proof of the existence of dark matter", *Astrophys. J.* **648** (2006) L109, doi:10.1086/508162, arXiv:astro-ph/0608407.

[4] DES Collaboration, "Dark Energy Survey year 1 results: curved-sky weak lensing mass map", *Mon. Not. Roy. Astron. Soc.* **475** (2018) 3165, doi:10.1093/mnras/stx3363, arXiv:1708.01535.

[5] Planck Collaboration, "Planck 2018 results. VI. Cosmological parameters", *Astron. Astrophys.* **641** (2020) A6, doi:10.1051/0004-6361/201833910, arXiv:1807.06209. [Erratum: doi:10.1051/0004-6361/201833910e].

[6] M. J. Strassler and K. M. Zurek, "Echoes of a hidden valley at hadron colliders", *Phys. Lett. B* **651** (2007) 374, doi:10.1016/j.physletb.2007.06.055, arXiv:hep-ph/0604261.

[7] K. Petraki and R. R. Volkas, "Review of asymmetric dark matter", *Int. J. Mod. Phys. A* **28** (2013) 1330028, doi:10.1142/S0217751X13300287, arXiv:1305.4939.

[8] H. Beauchesne, E. Bertuzzo, and G. Grilli di Cortona, "Dark matter in Hidden Valley models with stable and unstable light dark mesons", *JHEP* **04** (2019) 118, doi:10.1007/JHEP04(2019)118, arXiv:1809.10152.

[9] Y. Bai and P. Schwaller, "Scale of dark QCD", *Phys. Rev. D* **89** (2014) 063522, doi:10.1103/PhysRevD.89.063522, arXiv:1306.4676.

[10] T. Cohen, M. Lisanti, and H. K. Lou, "Semi-visible jets: Dark matter undercover at the LHC", *Phys. Rev. Lett.* **115** (2015) 171804, doi:10.1103/PhysRevLett.115.171804, arXiv:1503.00009.

[11] P. Schwaller, D. Stolarski, and A. Weiler, "Emerging jets", *JHEP* **05** (2015) 059, doi:10.1007/JHEP05(2015)059, arXiv:1502.05409.

[12] P. Agrawal, M. Blanke, and K. Gemmler, "Flavored dark matter beyond Minimal Flavor Violation", *JHEP* **10** (2014) 072, doi:10.1007/JHEP10(2014)072, arXiv:1405.6709.

[13] S. Renner and P. Schwaller, "A flavoured dark sector", *JHEP* **08** (2018) 052, doi:10.1007/JHEP08(2018)052, arXiv:1803.08080.

[14] P. Fayet and S. Ferrara, "Supersymmetry", *Phys. Rept.* **32** (1977) 249, doi:10.1016/0370-1573(77)90066-7.

[15] C. Borschensky et al., "Squark and gluino production cross sections in pp collisions at $\sqrt{s}$ = 13, 14, 33 and 100 TeV", *Eur. Phys. J. C* **74** (2014) 3174, doi:10.1140/epjc/s10052-014-3174-y, arXiv:1407.5066.

[16] W. Beenakker et al., "NNLL-fast: predictions for coloured supersymmetric particle production at the LHC with threshold and Coulomb resummation", *JHEP* **12** (2016) 133, doi:10.1007/JHEP12(2016)133, arXiv:1607.07741.

[17] CMS Collaboration, "Search for resonant production of strongly coupled dark matter in proton-proton collisions at 13 TeV", *JHEP* **06** (2022) 156, doi:10.1007/JHEP06(2022)156, arXiv:2112.11125.

[18] ATLAS Collaboration, "Search for non-resonant production of semi-visible jets using Run 2 data in ATLAS", *Phys. Lett. B* **848** (2024) 138324, doi:10.1016/j.physletb.2023.138324, arXiv:2305.18037.

[19] ATLAS Collaboration, "Search for resonant production of dark quarks in the dijet final state with the ATLAS detector", *JHEP* **02** (2024) 128, doi:10.1007/JHEP02(2024)128, arXiv:2311.03944.

[20] CMS Collaboration, "Search for new particles decaying to a jet and an emerging jet", *JHEP* **02** (2019) 179, doi:10.1007/JHEP02(2019)179, arXiv:1810.10069.

[21] HEPData record for this analysis, 2024. doi:10.17182/hepdata.147271.

[22] CMS Collaboration, "Description and performance of track and primary-vertex reconstruction with the CMS tracker", *JINST* **9** (2014) P10009, doi:10.1088/1748-0221/9/10/P10009, arXiv:1405.6569.

[23] Tracker Group of the CMS Collaboration, "The CMS phase-1 pixel detector upgrade", *JINST* **16** (2021) P02027, doi:10.1088/1748-0221/16/02/P02027, arXiv:2012.14304.

[24] CMS Collaboration, "Track impact parameter resolution for the full pseudo rapidity coverage in the 2017 dataset with the CMS phase-1 pixel detector", CMS Detector Performance Note CMS-DP-2020-049, 2020.

[25] CMS Collaboration, "Performance of the CMS Level-1 trigger in proton-proton collisions at $\sqrt{s} = 13\,\text{TeV}$", *JINST* **15** (2020) P10017, doi:10.1088/1748-0221/15/10/P10017, arXiv:2006.10165.

[26] CMS Collaboration, "The CMS trigger system", *JINST* **12** (2017) P01020, doi:10.1088/1748-0221/12/01/P01020, arXiv:1609.02366.

[27] CMS Collaboration, "The CMS experiment at the CERN LHC", *JINST* **3** (2008) S08004, doi:10.1088/1748-0221/3/08/S08004.

[28] L. Carloni and T. Sjöstrand, "Visible effects of invisible hidden valley radiation", *JHEP* **09** (2010) 105, doi:10.1007/JHEP09(2010)105, arXiv:1006.2911.

[29] L. Carloni, J. Rathsman, and T. Sjöstrand, "Discerning secluded sector gauge structures", *JHEP* **04** (2011) 091, doi:10.1007/JHEP04(2011)091, arXiv:1102.3795.

[30] T. Sjöstrand et al., "An introduction to PYTHIA 8.2", *Comput. Phys. Commun.* **191** (2015) 159, doi:10.1016/j.cpc.2015.01.024, arXiv:1410.3012.

[31] J. Alwall et al., "The automated computation of tree-level and next-to-leading order differential cross sections, and their matching to parton shower simulations", *JHEP* **07** (2014) 079, doi:10.1007/JHEP07(2014)079, arXiv:1405.0301.

[32] J. Alwall et al., "Comparative study of various algorithms for the merging of parton showers and matrix elements in hadronic collisions", *Eur. Phys. J. C* **53** (2008) 473, doi:10.1140/epjc/s10052-007-0490-5, arXiv:0706.2569.

[33] CMS Collaboration, "Extraction and validation of a new set of CMS PYTHIA8 tunes from underlying-event measurements", *Eur. Phys. J. C* **80** (2020) 4, doi:10.1140/epjc/s10052-019-7499-4, arXiv:1903.12179.

[34] NNPDF Collaboration, "Parton distributions from high-precision collider data", *Eur. Phys. J. C* **77** (2017) 663, doi:10.1140/epjc/s10052-017-5199-5, arXiv:1706.00428.

[35] GEANT4 Collaboration, "GEANT4—a simulation toolkit", *Nucl. Instrum. Meth. A* **506** (2003) 250, doi:10.1016/S0168-9002(03)01368-8.

[36] CMS Collaboration, "Particle-flow reconstruction and global event description with the CMS detector", *JINST* **12** (2017) P10003, doi:10.1088/1748-0221/12/10/P10003, arXiv:1706.04965.

[37] CMS Collaboration, "Performance of reconstruction and identification of τ leptons decaying to hadrons and ν_τ in pp collisions at $\sqrt{s} = 13$ TeV", *JINST* **13** (2018) P10005, doi:10.1088/1748-0221/13/10/P10005, arXiv:1809.02816.

[38] CMS Collaboration, "Jet energy scale and resolution in the CMS experiment in pp collisions at 8 TeV", *JINST* **12** (2017) P02014, doi:10.1088/1748-0221/12/02/P02014, arXiv:1607.03663.

[39] CMS Collaboration, "Performance of missing transverse momentum reconstruction in proton-proton collisions at $\sqrt{s} = 13$ TeV using the CMS detector", *JINST* **14** (2019) P07004, doi:10.1088/1748-0221/14/07/P07004, arXiv:1903.06078.

[40] M. Cacciari, G. P. Salam, and G. Soyez, "The anti-k_{T} jet clustering algorithm", *JHEP* **04** (2008) 063, doi:10.1088/1126-6708/2008/04/063, arXiv:0802.1189.

[41] M. Cacciari, G. P. Salam, and G. Soyez, "FastJet user manual", *Eur. Phys. J. C* **72** (2012) 1896, doi:10.1140/epjc/s10052-012-1896-2, arXiv:1111.6097.

[42] E. Bols et al., "Jet flavour classification using DeepJet", *JINST* **15** (2020) P12012, doi:10.1088/1748-0221/15/12/P12012, arXiv:2008.10519.

[43] CMS Collaboration, "Identification of heavy-flavour jets with the CMS detector in pp collisions at 13 TeV", *JINST* **13** (2018) P05011, doi:10.1088/1748-0221/13/05/P05011, arXiv:1712.07158.

[44] CMS Collaboration, "Performance summary of AK4 jet b tagging with data from proton-proton collisions at 13 TeV with the CMS detector", CMS Detector Performance Note CMS-DP-2023-005, 2023.

[45] K. Rose, "Deterministic annealing for clustering, compression, classification, regression, and related optimization problems", *IEEE Proc.* **86** (1998) 2210, doi:10.1109/5.726788.

[46] R. Fruhwirth, W. Waltenberger, and P. Vanlaer, "Adaptive vertex fitting", *J. Phys. G* **34** (2007) N343, doi:10.1088/0954-3899/34/12/N01.

[47] CMS Collaboration, "Technical proposal for the Phase-II upgrade of the Compact Muon Solenoid", CMS Technical Proposal CERN-LHCC-2015-010, CMS-TDR-15-02, 2015.

[48] CMS Collaboration, "Pileup mitigation at CMS in 13 TeV data", *JINST* **15** (2020) P09018, doi:10.1088/1748-0221/15/09/P09018, arXiv:2003.00503.

[49] CMS Collaboration, "Jet algorithms performance in 13 TeV data", CMS Physics Analysis Summary CMS-PAS-JME-16-003, 2017.

[50] J. Thaler and K. Van Tilburg, "Identifying boosted objects with N-subjettiness", *JHEP* **03** (2011) 015, doi:10.1007/JHEP03(2011)015, arXiv:1011.2268.

[51] H. Qu and L. Gouskos, "Jet tagging via particle clouds", *Phys. Rev. D* **101** (2020) 056019, doi:10.1103/PhysRevD.101.056019, arXiv:1902.08570.

[52] CMS Collaboration, "Precision luminosity measurement in proton-proton collisions at $\sqrt{s} = 13$ TeV in 2015 and 2016 at CMS", *Eur. Phys. J. C* **81** (2021) 800, doi:10.1140/epjc/s10052-021-09538-2, arXiv:2104.01927.

[53] CMS Collaboration, "CMS luminosity measurement for the 2017 data-taking period at $\sqrt{s} = 13$ TeV", CMS Physics Analysis Summary CMS-PAS-LUM-17-004, 2018.

[54] CMS Collaboration, "CMS luminosity measurement for the 2018 data-taking period at $\sqrt{s} = 13$ TeV", CMS Physics Analysis Summary CMS-PAS-LUM-18-002, 2019.

[55] CMS Collaboration, "Measurement of the inelastic proton-proton cross section at $\sqrt{s} = 13$ TeV", *JHEP* **07** (2018) 161, doi:10.1007/JHEP07(2018)161, arXiv:1802.02613.

[56] NNPDF Collaboration, "Parton distributions with QED corrections", *Nucl. Phys. B* **877** (2013) 290, doi:10.1016/j.nuclphysb.2013.10.010, arXiv:1308.0598.

[57] CMS Collaboration, "Muon tracking performance in the CMS Run-2 Legacy data using the tag-and-probe technique", CMS Detector Performance Note CMS-DP-2020-035, 2020.

[58] M. Cacciari et al., "The t anti-t cross-section at 1.8-TeV and 1.96-TeV: A study of the systematics due to parton densities and scale dependence", *JHEP* **04** (2004) 068, doi:10.1088/1126-6708/2004/04/068, arXiv:hep-ph/0303085.

[59] S. Catani, D. de Florian, M. Grazzini, and P. Nason, "Soft gluon resummation for Higgs boson production at hadron colliders", *JHEP* **07** (2003) 028, doi:10.1088/1126-6708/2003/07/028, arXiv:hep-ph/0306211.

[60] T. Junk, "Confidence level computation for combining searches with small statistics", *Nucl. Instrum. Meth. A* **434** (1999) 435, doi:10.1016/S0168-9002(99)00498-2, arXiv:hep-ex/9902006.

[61] A. L. Read, "Presentation of search results: the CL_s technique", *J. Phys. G* **28** (2002) 2693, doi:10.1088/0954-3899/28/10/313.

[62] ATLAS and CMS Collaborations, and LHC Higgs Combination Group, "Procedure for the LHC Higgs boson search combination in Summer 2011", Technical Report CMS-NOTE-2011-005, ATL-PHYS-PUB-2011-11, 2011.

A The CMS Collaboration

Yerevan Physics Institute, Yerevan, Armenia
A. Hayrapetyan, A. Tumasyan[1]

Institut für Hochenergiephysik, Vienna, Austria
W. Adam, J.W. Andrejkovic, T. Bergauer, S. Chatterjee, K. Damanakis, M. Dragicevic, P.S. Hussain, M. Jeitler[2], N. Krammer, A. Li, D. Liko, I. Mikulec, J. Schieck[2], R. Schöfbeck, D. Schwarz, M. Sonawane, S. Templ, W. Waltenberger, C.-E. Wulz[2]

Universiteit Antwerpen, Antwerpen, Belgium
M.R. Darwish[3], T. Janssen, P. Van Mechelen

Vrije Universiteit Brussel, Brussel, Belgium
N. Breugelmans, J. D'Hondt, S. Dansana, A. De Moor, M. Delcourt, F. Heyen, S. Lowette, I. Makarenko, D. Müller, S. Tavernier, M. Tytgat[4], G.P. Van Onsem, S. Van Putte, D. Vannerom

Université Libre de Bruxelles, Bruxelles, Belgium
B. Clerbaux, A.K. Das, G. De Lentdecker, H. Evard, L. Favart, P. Gianneios, D. Hohov, J. Jaramillo, A. Khalilzadeh, F.A. Khan, K. Lee, M. Mahdavikhorrami, A. Malara, S. Paredes, L. Thomas, M. Vanden Bemden, C. Vander Velde, P. Vanlaer

Ghent University, Ghent, Belgium
M. De Coen, D. Dobur, G. Gokbulut, Y. Hong, J. Knolle, L. Lambrecht, D. Marckx, G. Mestdach, K. Mota Amarilo, C. Rendón, A. Samalan, K. Skovpen, N. Van Den Bossche, J. van der Linden, L. Wezenbeek

Université Catholique de Louvain, Louvain-la-Neuve, Belgium
A. Benecke, A. Bethani, G. Bruno, C. Caputo, J. De Favereau De Jeneret, C. Delaere, I.S. Donertas, A. Giammanco, A.O. Guzel, Sa. Jain, V. Lemaitre, J. Lidrych, P. Mastrapasqua, T.T. Tran, S. Wertz

Centro Brasileiro de Pesquisas Fisicas, Rio de Janeiro, Brazil
G.A. Alves, E. Coelho, C. Hensel, T. Menezes De Oliveira, A. Moraes, P. Rebello Teles, M. Soeiro, A. Vilela Pereira[5]

Universidade do Estado do Rio de Janeiro, Rio de Janeiro, Brazil
W.L. Aldá Júnior, M. Alves Gallo Pereira, M. Barroso Ferreira Filho, H. Brandao Malbouisson, W. Carvalho, J. Chinellato[6], E.M. Da Costa, G.G. Da Silveira[7], D. De Jesus Damiao, S. Fonseca De Souza, R. Gomes De Souza, M. Macedo, J. Martins[8], C. Mora Herrera, L. Mundim, H. Nogima, J.P. Pinheiro, A. Santoro, A. Sznajder, M. Thiel

Universidade Estadual Paulista, Universidade Federal do ABC, São Paulo, Brazil
C.A. Bernardes[7], L. Calligaris, T.R. Fernandez Perez Tomei, E.M. Gregores, I. Maietto Silverio, P.G. Mercadante, S.F. Novaes, B. Orzari, Sandra S. Padula

Institute for Nuclear Research and Nuclear Energy, Bulgarian Academy of Sciences, Sofia, Bulgaria
A. Aleksandrov, G. Antchev, R. Hadjiiska, P. Iaydjiev, M. Misheva, M. Shopova, G. Sultanov

University of Sofia, Sofia, Bulgaria
A. Dimitrov, L. Litov, B. Pavlov, P. Petkov, A. Petrov, E. Shumka

Instituto De Alta Investigación, Universidad de Tarapacá, Casilla 7 D, Arica, Chile
S. Keshri, S. Thakur

Beihang University, Beijing, China
T. Cheng, T. Javaid, L. Yuan

Department of Physics, Tsinghua University, Beijing, China
Z. Hu, Z. Liang, J. Liu, K. Yi[9,10]

Institute of High Energy Physics, Beijing, China
G.M. Chen[11], H.S. Chen[11], M. Chen[11], F. Iemmi, C.H. Jiang, A. Kapoor[12], H. Liao, Z.-A. Liu[13], R. Sharma[14], J.N. Song[13], J. Tao, C. Wang[11], J. Wang, Z. Wang[11], H. Zhang, J. Zhao

State Key Laboratory of Nuclear Physics and Technology, Peking University, Beijing, China
A. Agapitos, Y. Ban, S. Deng, B. Guo, C. Jiang, A. Levin, C. Li, Q. Li, Y. Mao, S. Qian, S.J. Qian, X. Qin, X. Sun, D. Wang, H. Yang, L. Zhang, Y. Zhao, C. Zhou

Guangdong Provincial Key Laboratory of Nuclear Science and Guangdong-Hong Kong Joint Laboratory of Quantum Matter, South China Normal University, Guangzhou, China
S. Yang

Sun Yat-Sen University, Guangzhou, China
Z. You

University of Science and Technology of China, Hefei, China
K. Jaffel, N. Lu

Nanjing Normal University, Nanjing, China
G. Bauer[15], B. Li, J. Zhang

Institute of Modern Physics and Key Laboratory of Nuclear Physics and Ion-beam Application (MOE) - Fudan University, Shanghai, China
X. Gao[16]

Zhejiang University, Hangzhou, Zhejiang, China
Z. Lin, C. Lu, M. Xiao

Universidad de Los Andes, Bogota, Colombia
C. Avila, D.A. Barbosa Trujillo, A. Cabrera, C. Florez, J. Fraga, J.A. Reyes Vega

Universidad de Antioquia, Medellin, Colombia
F. Ramirez, M. Rodriguez, A.A. Ruales Barbosa, J.D. Ruiz Alvarez

University of Split, Faculty of Electrical Engineering, Mechanical Engineering and Naval Architecture, Split, Croatia
D. Giljanovic, N. Godinovic, D. Lelas, A. Sculac

University of Split, Faculty of Science, Split, Croatia
M. Kovac, A. Petkovic, T. Sculac

Institute Rudjer Boskovic, Zagreb, Croatia
P. Bargassa, V. Brigljevic, B.K. Chitroda, D. Ferencek, K. Jakovcic, S. Mishra, A. Starodumov[17], T. Susa

University of Cyprus, Nicosia, Cyprus
A. Attikis, K. Christoforou, A. Hadjiagapiou, C. Leonidou, J. Mousa, C. Nicolaou, L. Paizanos, F. Ptochos, P.A. Razis, H. Rykaczewski, H. Saka, A. Stepennov

Charles University, Prague, Czech Republic
M. Finger, M. Finger Jr., A. Kveton

Universidad San Francisco de Quito, Quito, Ecuador
E. Carrera Jarrin

Academy of Scientific Research and Technology of the Arab Republic of Egypt, Egyptian Network of High Energy Physics, Cairo, Egypt
Y. Assran[18,19], B. El-mahdy, S. Elgammal[19]

Center for High Energy Physics (CHEP-FU), Fayoum University, El-Fayoum, Egypt
M.A. Mahmoud, Y. Mohammed

National Institute of Chemical Physics and Biophysics, Tallinn, Estonia
K. Ehataht, M. Kadastik, T. Lange, S. Nandan, C. Nielsen, J. Pata, M. Raidal, L. Tani, C. Veelken

Department of Physics, University of Helsinki, Helsinki, Finland
H. Kirschenmann, K. Osterberg, M. Voutilainen

Helsinki Institute of Physics, Helsinki, Finland
S. Bharthuar, E. Brücken, F. Garcia, P. Inkaew, K.T.S. Kallonen, R. Kinnunen, T. Lampén, K. Lassila-Perini, S. Lehti, T. Lindén, L. Martikainen, M. Myllymäki, M.m. Rantanen, H. Siikonen, J. Tuominiemi

Lappeenranta-Lahti University of Technology, Lappeenranta, Finland
P. Luukka, H. Petrow

IRFU, CEA, Université Paris-Saclay, Gif-sur-Yvette, France
M. Besancon, F. Couderc, M. Dejardin, D. Denegri, J.L. Faure, F. Ferri, S. Ganjour, P. Gras, G. Hamel de Monchenault, V. Lohezic, J. Malcles, F. Orlandi, L. Portales, J. Rander, A. Rosowsky, M.Ö. Sahin, A. Savoy-Navarro[20], P. Simkina, M. Titov, M. Tornago

Laboratoire Leprince-Ringuet, CNRS/IN2P3, Ecole Polytechnique, Institut Polytechnique de Paris, Palaiseau, France
F. Beaudette, P. Busson, A. Cappati, C. Charlot, M. Chiusi, F. Damas, O. Davignon, A. De Wit, I.T. Ehle, B.A. Fontana Santos Alves, S. Ghosh, A. Gilbert, R. Granier de Cassagnac, A. Hakimi, B. Harikrishnan, L. Kalipoliti, G. Liu, M. Nguyen, C. Ochando, R. Salerno, J.B. Sauvan, Y. Sirois, E. Vernazza, A. Zabi, A. Zghiche

Université de Strasbourg, CNRS, IPHC UMR 7178, Strasbourg, France
J.-L. Agram[21], J. Andrea, D. Apparu, D. Bloch, J.-M. Brom, E.C. Chabert, C. Collard, S. Falke, U. Goerlach, R. Haeberle, A.-C. Le Bihan, M. Meena, O. Poncet, G. Saha, M.A. Sessini, P. Van Hove, P. Vaucelle

Institut de Physique des 2 Infinis de Lyon (IP2I), Villeurbanne, France
D. Amram, S. Beauceron, B. Blancon, G. Boudoul, N. Chanon, D. Contardo, P. Depasse, C. Dozen[22], H. El Mamouni, J. Fay, S. Gascon, M. Gouzevitch, C. Greenberg, G. Grenier, B. Ille, E. Jourd'huy, I.B. Laktineh, M. Lethuillier, L. Mirabito,

S. Perries, A. Purohit, M. Vander Donckt, P. Verdier, J. Xiao

Georgian Technical University, Tbilisi, Georgia
D. Chokheli, I. Lomidze, Z. Tsamalaidze[17]

RWTH Aachen University, I. Physikalisches Institut, Aachen, Germany
V. Botta, L. Feld, K. Klein, M. Lipinski, D. Meuser, A. Pauls, N. Röwert, M. Teroerde

RWTH Aachen University, III. Physikalisches Institut A, Aachen, Germany
S. Diekmann, A. Dodonova, N. Eich, D. Eliseev, F. Engelke, J. Erdmann, M. Erdmann, P. Fackeldey, B. Fischer, T. Hebbeker, K. Hoepfner, F. Ivone, A. Jung, M.y. Lee, F. Mausolf, M. Merschmeyer, A. Meyer, S. Mukherjee, D. Noll, F. Nowotny, A. Pozdnyakov, Y. Rath, W. Redjeb, F. Rehm, H. Reithler, V. Sarkisovi, A. Schmidt, A. Sharma, J.L. Spah, A. Stein, F. Torres Da Silva De Araujo[23], S. Wiedenbeck, S. Zaleski

RWTH Aachen University, III. Physikalisches Institut B, Aachen, Germany
C. Dziwok, G. Flügge, T. Kress, A. Nowack, O. Pooth, A. Stahl, T. Ziemons, A. Zotz

Deutsches Elektronen-Synchrotron, Hamburg, Germany
H. Aarup Petersen, M. Aldaya Martin, J. Alimena, S. Amoroso, Y. An, J. Bach, S. Baxter, M. Bayatmakou, H. Becerril Gonzalez, O. Behnke, A. Belvedere, S. Bhattacharya, F. Blekman[24], K. Borras[25], A. Campbell, A. Cardini, C. Cheng, F. Colombina, S. Consuegra Rodríguez, G. Correia Silva, M. De Silva, G. Eckerlin, D. Eckstein, L.I. Estevez Banos, O. Filatov, E. Gallo[24], A. Geiser, V. Guglielmi, M. Guthoff, A. Hinzmann, L. Jeppe, B. Kaech, M. Kasemann, C. Kleinwort, R. Kogler, M. Komm, D. Krücker, W. Lange, D. Leyva Pernia, K. Lipka[26], W. Lohmann[27], F. Lorkowski, R. Mankel, I.-A. Melzer-Pellmann, M. Mendizabal Morentin, A.B. Meyer, G. Milella, K. Moral Figueroa, A. Mussgiller, L.P. Nair, J. Niedziela, A. Nürnberg, Y. Otarid, J. Park, D. Pérez Adán, E. Ranken, A. Raspereza, D. Rastorguev, J. Rübenach, L. Rygaard, A. Saggio, M. Scham[28,25], S. Schnake[25], P. Schütze, C. Schwanenberger[24], D. Selivanova, K. Sharko, M. Shchedrolosiev, D. Stafford, F. Vazzoler, A. Ventura Barroso, R. Walsh, D. Wang, Q. Wang, Y. Wen, K. Wichmann, L. Wiens[25], C. Wissing, Y. Yang, A. Zimermmane Castro Santos

University of Hamburg, Hamburg, Germany
A. Albrecht, S. Albrecht, M. Antonello, S. Bein, L. Benato, S. Bollweg, M. Bonanomi, P. Connor, K. El Morabit, Y. Fischer, E. Garutti, A. Grohsjean, J. Haller, H.R. Jabusch, G. Kasieczka, P. Keicher, R. Klanner, W. Korcari, T. Kramer, C.c. Kuo, V. Kutzner, F. Labe, J. Lange, A. Lobanov, C. Matthies, L. Moureaux, M. Mrowietz, A. Nigamova, Y. Nissan, A. Paasch, K.J. Pena Rodriguez, T. Quadfasel, B. Raciti, M. Rieger, D. Savoiu, J. Schindler, P. Schleper, M. Schröder, J. Schwandt, M. Sommerhalder, H. Stadie, G. Steinbrück, A. Tews, M. Wolf

Karlsruher Institut fuer Technologie, Karlsruhe, Germany
S. Brommer, M. Burkart, E. Butz, T. Chwalek, A. Dierlamm, A. Droll, N. Faltermann, M. Giffels, A. Gottmann, F. Hartmann[29], R. Hofsaess, M. Horzela, U. Husemann, J. Kieseler, M. Klute, R. Koppenhöfer, J.M. Lawhorn, M. Link, A. Lintuluoto, B. Maier, S. Maier, S. Mitra, M. Mormile, Th. Müller, M. Neukum,

M. Oh, E. Pfeffer, M. Presilla, G. Quast, K. Rabbertz, B. Regnery, N. Shadskiy, I. Shvetsov, H.J. Simonis, L. Sowa, L. Stockmeier, K. Tauqeer, M. Toms, N. Trevisani, R.F. Von Cube, M. Wassmer, S. Wieland, F. Wittig, R. Wolf, X. Zuo

Institute of Nuclear and Particle Physics (INPP), NCSR Demokritos, Aghia Paraskevi, Greece
G. Anagnostou, G. Daskalakis, A. Kyriakis, A. Papadopoulos[29], A. Stakia

National and Kapodistrian University of Athens, Athens, Greece
P. Kontaxakis, G. Melachroinos, Z. Painesis, A. Panagiotou, I. Papavergou, I. Paraskevas, N. Saoulidou, K. Theofilatos, E. Tziaferi, K. Vellidis, I. Zisopoulos

National Technical University of Athens, Athens, Greece
G. Bakas, T. Chatzistavrou, G. Karapostoli, K. Kousouris, I. Papakrivopoulos, E. Siamarkou, G. Tsipolitis, A. Zacharopoulou

University of Ioánnina, Ioánnina, Greece
K. Adamidis, I. Bestintzanos, I. Evangelou, C. Foudas, C. Kamtsikis, P. Katsoulis, P. Kokkas, P.G. Kosmoglou Kioseoglou, N. Manthos, I. Papadopoulos, J. Strologas

HUN-REN Wigner Research Centre for Physics, Budapest, Hungary
M. Bartók[30], C. Hajdu, D. Horvath[31,32], K. Márton, A.J. Rádl[33], F. Sikler, V. Veszpremi

MTA-ELTE Lendület CMS Particle and Nuclear Physics Group, Eötvös Loránd University, Budapest, Hungary
M. Csanád, K. Farkas, A. Fehérkuti[34], M.M.A. Gadallah[35], Á. Kadlecsik, P. Major, G. Pásztor, G.I. Veres

Faculty of Informatics, University of Debrecen, Debrecen, Hungary
P. Raics, B. Ujvari, G. Zilizi

Institute of Nuclear Research ATOMKI, Debrecen, Hungary
G. Bencze, S. Czellar, J. Molnar, Z. Szillasi

Karoly Robert Campus, MATE Institute of Technology, Gyongyos, Hungary
T. Csorgo[34], T. Novak

Panjab University, Chandigarh, India
J. Babbar, S. Bansal, S.B. Beri, V. Bhatnagar, G. Chaudhary, S. Chauhan, N. Dhingra[36], A. Kaur, A. Kaur, H. Kaur, M. Kaur, S. Kumar, K. Sandeep, T. Sheokand, J.B. Singh, A. Singla

University of Delhi, Delhi, India
A. Ahmed, A. Bhardwaj, A. Chhetri, B.C. Choudhary, A. Kumar, A. Kumar, M. Naimuddin, K. Ranjan, M.K. Saini, S. Saumya

Saha Institute of Nuclear Physics, HBNI, Kolkata, India
S. Baradia, S. Barman[37], S. Bhattacharya, S. Das Gupta, S. Dutta, S. Dutta, S. Sarkar

Indian Institute of Technology Madras, Madras, India
M.M. Ameen, P.K. Behera, S.C. Behera, S. Chatterjee, G. Dash, P. Jana, P. Kalbhor, S. Kamble, J.R. Komaragiri[38], D. Kumar[38], P.R. Pujahari, N.R. Saha, A. Sharma, A.K. Sikdar, R.K. Singh, P. Verma, S. Verma, A. Vijay

Tata Institute of Fundamental Research-A, Mumbai, India

S. Dugad, M. Kumar, G.B. Mohanty, B. Parida, M. Shelake, P. Suryadevara

Tata Institute of Fundamental Research-B, Mumbai, India
A. Bala, S. Banerjee, R.M. Chatterjee, M. Guchait, Sh. Jain, A. Jaiswal, S. Kumar, G. Majumder, K. Mazumdar, S. Parolia, A. Thachayath

National Institute of Science Education and Research, An OCC of Homi Bhabha National Institute, Bhubaneswar, Odisha, India
S. Bahinipati[39], C. Kar, D. Maity[40], P. Mal, T. Mishra, V.K. Muraleedharan Nair Bindhu[40], K. Naskar[40], A. Nayak[40], S. Nayak, K. Pal, P. Sadangi, S.K. Swain, S. Varghese[40], D. Vats[40]

Indian Institute of Science Education and Research (IISER), Pune, India
S. Acharya[41], A. Alpana, S. Dube, B. Gomber[41], P. Hazarika, B. Kansal, A. Laha, B. Sahu[41], S. Sharma, K.Y. Vaish

Isfahan University of Technology, Isfahan, Iran
H. Bakhshiansohi[42], A. Jafari[43], M. Zeinali[44]

Institute for Research in Fundamental Sciences (IPM), Tehran, Iran
S. Bashiri, S. Chenarani[45], S.M. Etesami, Y. Hosseini, M. Khakzad, E. Khazaie[46], M. Mohammadi Najafabadi, S. Tizchang

University College Dublin, Dublin, Ireland
M. Felcini, M. Grunewald

INFN Sezione di Bari[a], Università di Bari[b], Politecnico di Bari[c], Bari, Italy
M. Abbrescia[a,b], A. Colaleo[a,b], D. Creanza[a,c], B. D'Anzi[a,b], N. De Filippis[a,c], M. De Palma[a,b], A. Di Florio[a,c], L. Fiore[a], G. Iaselli[a,c], M. Louka[a,b], G. Maggi[a,c], M. Maggi[a], I. Margjeka[a,b], V. Mastrapasqua[a,b], S. My[a,b], S. Nuzzo[a,b], A. Pellecchia[a,b], A. Pompili[a,b], G. Pugliese[a,c], R. Radogna[a], D. Ramos[a], A. Ranieri[a], L. Silvestris[a], F.M. Simone[a,b], Ü. Sözbilir[a], A. Stamerra[a], D. Troiano[a], R. Venditti[a], P. Verwilligen[a], A. Zaza[a,b]

INFN Sezione di Bologna[a], Università di Bologna[b], Bologna, Italy
G. Abbiendi[a], C. Battilana[a,b], D. Bonacorsi[a,b], L. Borgonovi[a], P. Capiluppi[a,b], A. Castro[†a,b], F.R. Cavallo[a], M. Cuffiani[a,b], G.M. Dallavalle[a], T. Diotalevi[a,b], F. Fabbri[a], A. Fanfani[a,b], D. Fasanella[a,b], P. Giacomelli[a], L. Giommi[a,b], C. Grandi[a], L. Guiducci[a,b], S. Lo Meo[a,47], M. Lorusso[a,b], L. Lunerti[a], S. Marcellini[a], G. Masetti[a], F.L. Navarria[a,b], G. Paggi[a], A. Perrotta[a], F. Primavera[a,b], A.M. Rossi[a,b], S. Rossi Tisbeni[a,b], T. Rovelli[a,b], G.P. Siroli[a,b]

INFN Sezione di Catania[a], Università di Catania[b], Catania, Italy
S. Costa[a,b,48], A. Di Mattia[a], R. Potenza[a,b], A. Tricomi[a,b,48], C. Tuve[a,b]

INFN Sezione di Firenze[a], Università di Firenze[b], Firenze, Italy
P. Assiouras[a], G. Barbagli[a], G. Bardelli[a,b], B. Camaiani[a,b], A. Cassese[a], R. Ceccarelli[a], V. Ciulli[a,b], C. Civinini[a], R. D'Alessandro[a,b], E. Focardi[a,b], T. Kello[a], G. Latino[a,b], P. Lenzi[a,b], M. Lizzo[a], M. Meschini[a], S. Paoletti[a], A. Papanastassiou[a,b], G. Sguazzoni[a], L. Viliani[a]

INFN Laboratori Nazionali di Frascati, Frascati, Italy
L. Benussi, S. Bianco, S. Meola[49], D. Piccolo

INFN Sezione di Genova[a], Università di Genova[b], Genova, Italy

P. Chatagnon[a], F. Ferro[a], E. Robutti[a], S. Tosi[a,b]

INFN Sezione di Milano-Bicocca[a], Università di Milano-Bicocca[b], Milano, Italy
A. Benaglia[a], G. Boldrini[a,b], F. Brivio[a], F. Cetorelli[a], F. De Guio[a,b], M.E. Dinardo[a,b], P. Dini[a], S. Gennai[a], R. Gerosa[a,b], A. Ghezzi[a,b], P. Govoni[a,b], L. Guzzi[a], M.T. Lucchini[a,b], M. Malberti[a], S. Malvezzi[a], A. Massironi[a], D. Menasce[a], L. Moroni[a], M. Paganoni[a,b], S. Palluotto[a,b], D. Pedrini[a], A. Perego[a], B.S. Pinolini[a], G. Pizzati[a,b], S. Ragazzi[a,b], T. Tabarelli de Fatis[a,b]

INFN Sezione di Napoli[a], Università di Napoli 'Federico II'[b], Napoli, Italy; Università della Basilicata[c], Potenza, Italy; Scuola Superiore Meridionale (SSM)[d], Napoli, Italy
S. Buontempo[a], A. Cagnotta[a,b], F. Carnevali[a,b], N. Cavallo[a,c], F. Fabozzi[a,c], A.O.M. Iorio[a,b], L. Lista[a,b,50], P. Paolucci[a,29], B. Rossi[a], C. Sciacca[a,b]

INFN Sezione di Padova[a], Università di Padova[b], Padova, Italy; Università di Trento[c], Trento, Italy
R. Ardino[a], P. Azzi[a], N. Bacchetta[a,51], M. Bellato[a], D. Bisello[a,b], P. Bortignon[a], G. Bortolato[a,b], A. Bragagnolo[a,b], A.C.M. Bulla[a], R. Carlin[a,b], P. Checchia[a], T. Dorigo[a], F. Gasparini[a,b], U. Gasparini[a,b], E. Lusiani[a], M. Margoni[a,b], M. Migliorini[a,b], J. Pazzini[a,b], P. Ronchese[a,b], R. Rossin[a,b], F. Simonetto[a,b], G. Strong[a], M. Tosi[a,b], A. Triossi[a,b], S. Ventura[a], M. Zanetti[a,b], P. Zotto[a,b], A. Zucchetta[a,b], G. Zumerle[a,b]

INFN Sezione di Pavia[a], Università di Pavia[b], Pavia, Italy
C. Aimè[a], A. Braghieri[a], S. Calzaferri[a], D. Fiorina[a], P. Montagna[a,b], V. Re[a], C. Riccardi[a,b], P. Salvini[a], I. Vai[a,b], P. Vitulo[a,b]

INFN Sezione di Perugia[a], Università di Perugia[b], Perugia, Italy
S. Ajmal[a,b], M.E. Ascioti[a,b], G.M. Bilei[a], C. Carrivale[a,b], D. Ciangottini[a,b], L. Fanò[a,b], M. Magherini[a,b], V. Mariani[a,b], M. Menichelli[a], F. Moscatelli[a,52], A. Rossi[a,b], A. Santocchia[a,b], D. Spiga[a], T. Tedeschi[a,b]

INFN Sezione di Pisa[a], Università di Pisa[b], Scuola Normale Superiore di Pisa[c], Pisa, Italy; Università di Siena[d], Siena, Italy
C.A. Alexe[a,c], P. Asenov[a,b], P. Azzurri[a], G. Bagliesi[a], R. Bhattacharya[a], L. Bianchini[a,b], T. Boccali[a], E. Bossini[a], D. Bruschini[a,c], R. Castaldi[a], M.A. Ciocci[a,b], M. Cipriani[a,b], V. D'Amante[a,d], R. Dell'Orso[a], S. Donato[a], A. Giassi[a], F. Ligabue[a,c], D. Matos Figueiredo[a], A. Messineo[a,b], M. Musich[a,b], F. Palla[a], A. Rizzi[a,b], G. Rolandi[a,c], S. Roy Chowdhury[a], T. Sarkar[a], A. Scribano[a], P. Spagnolo[a], R. Tenchini[a], G. Tonelli[a,b], N. Turini[a,d], F. Vaselli[a,c], A. Venturi[a], P.G. Verdini[a]

INFN Sezione di Roma[a], Sapienza Università di Roma[b], Roma, Italy
C. Baldenegro Barrera[a,b], P. Barria[a], C. Basile[a,b], M. Campana[a,b], F. Cavallari[a], L. Cunqueiro Mendez[a,b], D. Del Re[a,b], E. Di Marco[a], M. Diemoz[a], F. Errico[a,b], E. Longo[a,b], P. Meridiani[a], J. Mijuskovic[a,b], G. Organtini[a,b], F. Pandolfi[a], R. Paramatti[a,b], C. Quaranta[a,b], S. Rahatlou[a,b], C. Rovelli[a], F. Santanastasio[a,b], L. Soffi[a]

INFN Sezione di Torino[a], Università di Torino[b], Torino, Italy; Università del Piemonte Orientale[c], Novara, Italy
N. Amapane[a,b], R. Arcidiacono[a,c], S. Argiro[a,b], M. Arneodo[a,c], N. Bartosik[a], R. Bellan[a,b], A. Bellora[a,b], C. Biino[a], C. Borca[a,b], N. Cartiglia[a], M. Costa[a,b],

R. Covarelli[a,b], N. Demaria[a], L. Finco[a], M. Grippo[a,b], B. Kiani[a,b], F. Legger[a], F. Luongo[a,b], C. Mariotti[a], L. Markovic[a,b], S. Maselli[a], A. Mecca[a,b], L. Menzio[a,b], E. Migliore[a,b], M. Monteno[a], R. Mulargia[a], M.M. Obertino[a,b], G. Ortona[a], L. Pacher[a,b], N. Pastrone[a], M. Pelliccioni[a], M. Ruspa[a,c], F. Siviero[a,b], V. Sola[a,b], A. Solano[a,b], A. Staiano[a], C. Tarricone[a,b], D. Trocino[a], G. Umoret[a,b], E. Vlasov[a,b], R. White[a,b]

INFN Sezione di Trieste[a], Università di Trieste[b], Trieste, Italy
S. Belforte[a], V. Candelise[a,b], M. Casarsa[a], F. Cossutti[a], K. De Leo[a], G. Della Ricca[a,b]

Kyungpook National University, Daegu, Korea
S. Dogra, J. Hong, C. Huh, B. Kim, J. Kim, D. Lee, H. Lee, S.W. Lee, C.S. Moon, Y.D. Oh, M.S. Ryu, S. Sekmen, B. Tae, Y.C. Yang

Department of Mathematics and Physics - GWNU, Gangneung, Korea
M.S. Kim

Chonnam National University, Institute for Universe and Elementary Particles, Kwangju, Korea
G. Bak, P. Gwak, H. Kim, D.H. Moon

Hanyang University, Seoul, Korea
E. Asilar, J. Choi, D. Kim, T.J. Kim, J.A. Merlin, Y. Ryou

Korea University, Seoul, Korea
S. Choi, S. Han, B. Hong, K. Lee, K.S. Lee, S. Lee, S.K. Park, J. Yoo

Kyung Hee University, Department of Physics, Seoul, Korea
J. Goh, S. Yang

Sejong University, Seoul, Korea
H. S. Kim, Y. Kim, S. Lee

Seoul National University, Seoul, Korea
J. Almond, J.H. Bhyun, J. Choi, J. Choi, W. Jun, J. Kim, S. Ko, H. Kwon, H. Lee, J. Lee, J. Lee, B.H. Oh, S.B. Oh, H. Seo, U.K. Yang, I. Yoon

University of Seoul, Seoul, Korea
W. Jang, D.Y. Kang, Y. Kang, S. Kim, B. Ko, J.S.H. Lee, Y. Lee, I.C. Park, Y. Roh, I.J. Watson

Yonsei University, Department of Physics, Seoul, Korea
S. Ha, H.D. Yoo

Sungkyunkwan University, Suwon, Korea
M. Choi, M.R. Kim, H. Lee, Y. Lee, I. Yu

College of Engineering and Technology, American University of the Middle East (AUM), Dasman, Kuwait
T. Beyrouthy

Riga Technical University, Riga, Latvia
K. Dreimanis, A. Gaile, G. Pikurs, A. Potrebko, M. Seidel, D. Sidiropoulos Kontos

University of Latvia (LU), Riga, Latvia
N.R. Strautnieks

Vilnius University, Vilnius, Lithuania
M. Ambrozas, A. Juodagalvis, A. Rinkevicius, G. Tamulaitis

National Centre for Particle Physics, Universiti Malaya, Kuala Lumpur, Malaysia
N. Bin Norjoharuddeen, I. Yusuff[53], Z. Zolkapli

Universidad de Sonora (UNISON), Hermosillo, Mexico
J.F. Benitez, A. Castaneda Hernandez, H.A. Encinas Acosta, L.G. Gallegos Maríñez, M. León Coello, J.A. Murillo Quijada, A. Sehrawat, L. Valencia Palomo

Centro de Investigacion y de Estudios Avanzados del IPN, Mexico City, Mexico
G. Ayala, H. Castilla-Valdez, H. Crotte Ledesma, E. De La Cruz-Burelo, I. Heredia-De La Cruz[54], R. Lopez-Fernandez, J. Mejia Guisao, C.A. Mondragon Herrera, A. Sánchez Hernández

Universidad Iberoamericana, Mexico City, Mexico
C. Oropeza Barrera, D.L. Ramirez Guadarrama, M. Ramírez García

Benemerita Universidad Autonoma de Puebla, Puebla, Mexico
I. Bautista, I. Pedraza, H.A. Salazar Ibarguen, C. Uribe Estrada

University of Montenegro, Podgorica, Montenegro
I. Bubanja, N. Raicevic

University of Canterbury, Christchurch, New Zealand
P.H. Butler

National Centre for Physics, Quaid-I-Azam University, Islamabad, Pakistan
A. Ahmad, M.I. Asghar, A. Awais, M.I.M. Awan, H.R. Hoorani, W.A. Khan

AGH University of Krakow, Faculty of Computer Science, Electronics and Telecommunications, Krakow, Poland
V. Avati, L. Grzanka, M. Malawski

National Centre for Nuclear Research, Swierk, Poland
H. Bialkowska, M. Bluj, M. Górski, M. Kazana, M. Szleper, P. Zalewski

Institute of Experimental Physics, Faculty of Physics, University of Warsaw, Warsaw, Poland
K. Bunkowski, K. Doroba, A. Kalinowski, M. Konecki, J. Krolikowski, A. Muhammad

Warsaw University of Technology, Warsaw, Poland
K. Pozniak, W. Zabolotny

Laboratório de Instrumentação e Física Experimental de Partículas, Lisboa, Portugal
M. Araujo, D. Bastos, C. Beirão Da Cruz E Silva, A. Boletti, M. Bozzo, T. Camporesi, G. Da Molin, P. Faccioli, M. Gallinaro, J. Hollar, N. Leonardo, G.B. Marozzo, T. Niknejad, A. Petrilli, M. Pisano, J. Seixas, J. Varela, J.W. Wulff

Faculty of Physics, University of Belgrade, Belgrade, Serbia
P. Adzic, P. Milenovic

VINCA Institute of Nuclear Sciences, University of Belgrade, Belgrade, Serbia
M. Dordevic, J. Milosevic, L. Nadderd, V. Rekovic

Centro de Investigaciones Energéticas Medioambientales y Tecnológicas (CIEMAT), Madrid, Spain

J. Alcaraz Maestre, Cristina F. Bedoya, Oliver M. Carretero, M. Cepeda, M. Cerrada, N. Colino, B. De La Cruz, A. Delgado Peris, A. Escalante Del Valle, D. Fernández Del Val, J.P. Fernández Ramos, J. Flix, M.C. Fouz, O. Gonzalez Lopez, S. Goy Lopez, J.M. Hernandez, M.I. Josa, E. Martin Viscasillas, D. Moran, C. M. Morcillo Perez, Á. Navarro Tobar, C. Perez Dengra, A. Pérez-Calero Yzquierdo, J. Puerta Pelayo, I. Redondo, S. Sánchez Navas, J. Sastre, L. Urda Gómez, J. Vazquez Escobar

Universidad Autónoma de Madrid, Madrid, Spain
J.F. de Trocóniz

Universidad de Oviedo, Instituto Universitario de Ciencias y Tecnologías Espaciales de Asturias (ICTEA), Oviedo, Spain
B. Alvarez Gonzalez, J. Cuevas, J. Fernandez Menendez, S. Folgueras, I. Gonzalez Caballero, J.R. González Fernández, P. Leguina, E. Palencia Cortezon, C. Ramón Álvarez, V. Rodríguez Bouza, A. Soto Rodríguez, A. Trapote, C. Vico Villalba, P. Vischia

Instituto de Física de Cantabria (IFCA), CSIC-Universidad de Cantabria, Santander, Spain
S. Bhowmik, S. Blanco Fernández, J.A. Brochero Cifuentes, I.J. Cabrillo, A. Calderon, J. Duarte Campderros, M. Fernandez, G. Gomez, C. Lasaosa García, R. Lopez Ruiz, C. Martinez Rivero, P. Martinez Ruiz del Arbol, F. Matorras, P. Matorras Cuevas, E. Navarrete Ramos, J. Piedra Gomez, L. Scodellaro, I. Vila, J.M. Vizan Garcia

University of Colombo, Colombo, Sri Lanka
B. Kailasapathy[55], D.D.C. Wickramarathna

University of Ruhuna, Department of Physics, Matara, Sri Lanka
W.G.D. Dharmaratna[56], K. Liyanage, N. Perera

CERN, European Organization for Nuclear Research, Geneva, Switzerland
D. Abbaneo, C. Amendola, E. Auffray, G. Auzinger, J. Baechler, D. Barney, A. Bermúdez Martínez, M. Bianco, B. Bilin, A.A. Bin Anuar, A. Bocci, C. Botta, E. Brondolin, C. Caillol, G. Cerminara, N. Chernyavskaya, D. d'Enterria, A. Dabrowski, A. David, A. De Roeck, M.M. Defranchis, M. Deile, M. Dobson, G. Franzoni, W. Funk, S. Giani, D. Gigi, K. Gill, F. Glege, L. Gouskos, J. Hegeman, J.K. Heikkilä, B. Huber, V. Innocente, T. James, P. Janot, O. Kaluzinska, S. Laurila, P. Lecoq, E. Leutgeb, C. Lourenço, L. Malgeri, M. Mannelli, A.C. Marini, M. Matthewman, A. Mehta, F. Meijers, S. Mersi, E. Meschi, V. Milosevic, F. Monti, F. Moortgat, M. Mulders, I. Neutelings, S. Orfanelli, F. Pantaleo, G. Petrucciani, A. Pfeiffer, M. Pierini, H. Qu, D. Rabady, B. Ribeiro Lopes, M. Rovere, H. Sakulin, S. Sanchez Cruz, S. Scarfi, C. Schwick, M. Selvaggi, A. Sharma, K. Shchelina, P. Silva, P. Sphicas[57], A.G. Stahl Leiton, A. Steen, S. Summers, D. Treille, P. Tropea, D. Walter, J. Wanczyk[58], J. Wang, S. Wuchterl, P. Zehetner, P. Zejdl, W.D. Zeuner

Paul Scherrer Institut, Villigen, Switzerland
T. Bevilacqua[59], L. Caminada[59], A. Ebrahimi, W. Erdmann, R. Horisberger, Q. Ingram, H.C. Kaestli, D. Kotlinski, C. Lange, M. Missiroli[59], L. Noehte[59], T. Rohe

ETH Zurich - Institute for Particle Physics and Astrophysics (IPA), Zurich, Switzerland

T.K. Aarrestad, K. Androsov[58], M. Backhaus, G. Bonomelli, A. Calandri, C. Cazzaniga, K. Datta, P. De Bryas Dexmiers D'archiac[58], A. De Cosa, G. Dissertori, M. Dittmar, M. Donegà, F. Eble, M. Galli, K. Gedia, F. Glessgen, C. Grab, N. Härringer, T.G. Harte, D. Hits, W. Lustermann, A.-M. Lyon, R.A. Manzoni, M. Marchegiani, L. Marchese, C. Martin Perez, A. Mascellani[58], F. Nessi-Tedaldi, F. Pauss, V. Perovic, S. Pigazzini, C. Reissel, T. Reitenspiess, B. Ristic, F. Riti, R. Seidita, J. Steggemann[58], A. Tarabini, D. Valsecchi, R. Wallny

Universität Zürich, Zurich, Switzerland
C. Amsler[60], P. Bärtschi, M.F. Canelli, K. Cormier, M. Huwiler, W. Jin, A. Jofrehei, B. Kilminster, S. Leontsinis, S.P. Liechti, A. Macchiolo, P. Meiring, F. Meng, U. Molinatti, J. Motta, A. Reimers, P. Robmann, M. Senger, E. Shokr, F. Stäger, R. Tramontano

National Central University, Chung-Li, Taiwan
C. Adloff[61], D. Bhowmik, C.M. Kuo, W. Lin, P.K. Rout, P.C. Tiwari[38], S.S. Yu

National Taiwan University (NTU), Taipei, Taiwan
L. Ceard, K.F. Chen, P.s. Chen, Z.g. Chen, A. De Iorio, W.-S. Hou, T.h. Hsu, Y.w. Kao, S. Karmakar, G. Kole, Y.y. Li, R.-S. Lu, E. Paganis, X.f. Su, J. Thomas-Wilsker, L.s. Tsai, H.y. Wu, E. Yazgan

High Energy Physics Research Unit, Department of Physics, Faculty of Science, Chulalongkorn University, Bangkok, Thailand
C. Asawatangtrakuldee, N. Srimanobhas, V. Wachirapusitanand

Çukurova University, Physics Department, Science and Art Faculty, Adana, Turkey
D. Agyel, F. Boran, F. Dolek, I. Dumanoglu[62], E. Eskut, Y. Guler[63], E. Gurpinar Guler[63], C. Isik, O. Kara, A. Kayis Topaksu, U. Kiminsu, G. Onengut, K. Ozdemir[64], A. Polatoz, B. Tali[65], U.G. Tok, S. Turkcapar, E. Uslan, I.S. Zorbakir

Middle East Technical University, Physics Department, Ankara, Turkey
G. Sokmen, M. Yalvac[66]

Bogazici University, Istanbul, Turkey
B. Akgun, I.O. Atakisi, E. Gülmez, M. Kaya[67], O. Kaya[68], S. Tekten[69]

Istanbul Technical University, Istanbul, Turkey
A. Cakir, K. Cankocak[62,70], G.G. Dincer[62], Y. Komurcu, S. Sen[71]

Istanbul University, Istanbul, Turkey
O. Aydilek[72], V. Epshteyn, B. Hacisahinoglu, I. Hos[73], B. Kaynak, S. Ozkorucuklu, O. Potok, H. Sert, C. Simsek, C. Zorbilmez

Yildiz Technical University, Istanbul, Turkey
S. Cerci[65], B. Isildak[74], D. Sunar Cerci, T. Yetkin

Institute for Scintillation Materials of National Academy of Science of Ukraine, Kharkiv, Ukraine
A. Boyaryntsev, B. Grynyov

National Science Centre, Kharkiv Institute of Physics and Technology, Kharkiv, Ukraine
L. Levchuk

University of Bristol, Bristol, United Kingdom

D. Anthony, J.J. Brooke, A. Bundock, F. Bury, E. Clement, D. Cussans, H. Flacher, M. Glowacki, J. Goldstein, H.F. Heath, M.-L. Holmberg, L. Kreczko, S. Paramesvaran, L. Robertshaw, S. Seif El Nasr-Storey, V.J. Smith, N. Stylianou[75], K. Walkingshaw Pass

Rutherford Appleton Laboratory, Didcot, United Kingdom
A.H. Ball, K.W. Bell, A. Belyaev[76], C. Brew, R.M. Brown, D.J.A. Cockerill, C. Cooke, A. Elliot, K.V. Ellis, K. Harder, S. Harper, J. Linacre, K. Manolopoulos, D.M. Newbold, E. Olaiya, D. Petyt, T. Reis, A.R. Sahasransu, G. Salvi, T. Schuh, C.H. Shepherd-Themistocleous, I.R. Tomalin, K.C. Whalen, T. Williams

Imperial College, London, United Kingdom
R. Bainbridge, P. Bloch, C.E. Brown, O. Buchmuller, V. Cacchio, C.A. Carrillo Montoya, G.S. Chahal[77], D. Colling, J.S. Dancu, I. Das, P. Dauncey, G. Davies, J. Davies, M. Della Negra, S. Fayer, G. Fedi, G. Hall, M.H. Hassanshahi, A. Howard, G. Iles, M. Knight, J. Langford, J. León Holgado, L. Lyons, A.-M. Magnan, S. Mallios, M. Mieskolainen, J. Nash[78], M. Pesaresi, P.B. Pradeep, B.C. Radburn-Smith, A. Richards, A. Rose, K. Savva, C. Seez, R. Shukla, A. Tapper, K. Uchida, G.P. Uttley, L.H. Vage, T. Virdee[29], M. Vojinovic, N. Wardle, D. Winterbottom

Brunel University, Uxbridge, United Kingdom
K. Coldham, J.E. Cole, A. Khan, P. Kyberd, I.D. Reid

Baylor University, Waco, Texas, USA
S. Abdullin, A. Brinkerhoff, B. Caraway, E. Collins, J. Dittmann, K. Hatakeyama, J. Hiltbrand, B. McMaster, J. Samudio, S. Sawant, C. Sutantawibul, J. Wilson

Catholic University of America, Washington, DC, USA
R. Bartek, A. Dominguez, C. Huerta Escamilla, A.E. Simsek, R. Uniyal, A.M. Vargas Hernandez

The University of Alabama, Tuscaloosa, Alabama, USA
B. Bam, A. Buchot Perraguin, R. Chudasama, S.I. Cooper, C. Crovella, S.V. Gleyzer, E. Pearson, C.U. Perez, P. Rumerio[79], E. Usai, R. Yi

Boston University, Boston, Massachusetts, USA
A. Akpinar, C. Cosby, G. De Castro, Z. Demiragli, C. Erice, C. Fangmeier, C. Fernandez Madrazo, E. Fontanesi, D. Gastler, F. Golf, S. Jeon, J. O'cain, I. Reed, J. Rohlf, K. Salyer, D. Sperka, D. Spitzbart, I. Suarez, A. Tsatsos, A.G. Zecchinelli

Brown University, Providence, Rhode Island, USA
G. Benelli, X. Coubez[25], D. Cutts, M. Hadley, U. Heintz, J.M. Hogan[80], T. Kwon, G. Landsberg, K.T. Lau, D. Li, J. Luo, S. Mondal, M. Narain[†], N. Pervan, S. Sagir[81], F. Simpson, M. Stamenkovic, N. Venkatasubramanian, X. Yan, W. Zhang

University of California, Davis, Davis, California, USA
S. Abbott, J. Bonilla, C. Brainerd, R. Breedon, H. Cai, M. Calderon De La Barca Sanchez, M. Chertok, M. Citron, J. Conway, P.T. Cox, R. Erbacher, F. Jensen, O. Kukral, G. Mocellin, M. Mulhearn, S. Ostrom, W. Wei, Y. Yao, S. Yoo, F. Zhang

University of California, Los Angeles, California, USA

M. Bachtis, R. Cousins, A. Datta, G. Flores Avila, J. Hauser, M. Ignatenko, M.A. Iqbal, T. Lam, E. Manca, A. Nunez Del Prado, D. Saltzberg, V. Valuev

University of California, Riverside, Riverside, California, USA
R. Clare, J.W. Gary, M. Gordon, G. Hanson, W. Si, S. Wimpenny[†]

University of California, San Diego, La Jolla, California, USA
A. Aportela, A. Arora, J.G. Branson, S. Cittolin, S. Cooperstein, D. Diaz, J. Duarte, L. Giannini, Y. Gu, J. Guiang, R. Kansal, V. Krutelyov, R. Lee, J. Letts, M. Masciovecchio, F. Mokhtar, S. Mukherjee, M. Pieri, M. Quinnan, B.V. Sathia Narayanan, V. Sharma, M. Tadel, E. Vourliotis, F. Würthwein, Y. Xiang, A. Yagil

University of California, Santa Barbara - Department of Physics, Santa Barbara, California, USA
A. Barzdukas, L. Brennan, C. Campagnari, K. Downham, C. Grieco, J. Incandela, J. Kim, A.J. Li, P. Masterson, H. Mei, J. Richman, S.N. Santpur, U. Sarica, R. Schmitz, F. Setti, J. Sheplock, D. Stuart, T.Á. Vámi, S. Wang, D. Zhang

California Institute of Technology, Pasadena, California, USA
A. Bornheim, O. Cerri, A. Latorre, J. Mao, H.B. Newman, G. Reales Gutiérrez, M. Spiropulu, J.R. Vlimant, C. Wang, S. Xie, R.Y. Zhu

Carnegie Mellon University, Pittsburgh, Pennsylvania, USA
J. Alison, S. An, M.B. Andrews, P. Bryant, M. Cremonesi, V. Dutta, T. Ferguson, T.A. Gómez Espinosa, A. Harilal, A. Kallil Tharayil, C. Liu, T. Mudholkar, S. Murthy, P. Palit, K. Park, M. Paulini, A. Roberts, A. Sanchez, W. Terrill

University of Colorado Boulder, Boulder, Colorado, USA
J.P. Cumalat, W.T. Ford, A. Hart, A. Hassani, G. Karathanasis, N. Manganelli, J. Pearkes, A. Perloff, C. Savard, N. Schonbeck, K. Stenson, K.A. Ulmer, S.R. Wagner, N. Zipper, D. Zuolo

Cornell University, Ithaca, New York, USA
J. Alexander, S. Bright-Thonney, X. Chen, D.J. Cranshaw, J. Fan, X. Fan, S. Hogan, P. Kotamnives, J. Monroy, M. Oshiro, J.R. Patterson, M. Reid, A. Ryd, J. Thom, P. Wittich, R. Zou

Fermi National Accelerator Laboratory, Batavia, Illinois, USA
M. Albrow, M. Alyari, O. Amram, G. Apollinari, A. Apresyan, L.A.T. Bauerdick, D. Berry, J. Berryhill, P.C. Bhat, K. Burkett, J.N. Butler, A. Canepa, G.B. Cerati, H.W.K. Cheung, F. Chlebana, G. Cummings, J. Dickinson, I. Dutta, V.D. Elvira, Y. Feng, J. Freeman, A. Gandrakota, Z. Gecse, L. Gray, D. Green, A. Grummer, S. Grünendahl, D. Guerrero, O. Gutsche, R.M. Harris, R. Heller, T.C. Herwig, J. Hirschauer, B. Jayatilaka, S. Jindariani, M. Johnson, U. Joshi, T. Klijnsma, B. Klima, K.H.M. Kwok, S. Lammel, D. Lincoln, R. Lipton, T. Liu, C. Madrid, K. Maeshima, C. Mantilla, D. Mason, P. McBride, P. Merkel, S. Mrenna, S. Nahn, J. Ngadiuba, D. Noonan, S. Norberg, V. Papadimitriou, N. Pastika, K. Pedro, C. Pena[82], F. Ravera, A. Reinsvold Hall[83], L. Ristori, M. Safdari, E. Sexton-Kennedy, N. Smith, A. Soha, L. Spiegel, S. Stoynev, J. Strait, L. Taylor, S. Tkaczyk, N.V. Tran, L. Uplegger, E.W. Vaandering, I. Zoi

University of Florida, Gainesville, Florida, USA
C. Aruta, P. Avery, D. Bourilkov, P. Chang, V. Cherepanov, R.D. Field, E. Koenig,

M. Kolosova, J. Konigsberg, A. Korytov, K. Matchev, N. Menendez, G. Mitselmakher, K. Mohrman, A. Muthirakalayil Madhu, N. Rawal, S. Rosenzweig, Y. Takahashi, J. Wang

Florida State University, Tallahassee, Florida, USA
T. Adams, A. Al Kadhim, A. Askew, S. Bower, R. Habibullah, V. Hagopian, R. Hashmi, R.S. Kim, S. Kim, T. Kolberg, G. Martinez, H. Prosper, P.R. Prova, M. Wulansatiti, R. Yohay, J. Zhang

Florida Institute of Technology, Melbourne, Florida, USA
B. Alsufyani, M.M. Baarmand, S. Butalla, S. Das, T. Elkafrawy[84], M. Hohlmann, M. Rahmani, E. Yanes

University of Illinois Chicago, Chicago, USA, Chicago, USA
M.R. Adams, A. Baty, C. Bennett, R. Cavanaugh, R. Escobar Franco, O. Evdokimov, C.E. Gerber, M. Hawksworth, A. Hingrajiya, D.J. Hofman, J.h. Lee, D. S. Lemos, A.H. Merrit, C. Mills, S. Nanda, G. Oh, B. Ozek, D. Pilipovic, R. Pradhan, E. Prifti, T. Roy, S. Rudrabhatla, M.B. Tonjes, N. Varelas, M.A. Wadud, Z. Ye, J. Yoo

The University of Iowa, Iowa City, Iowa, USA
M. Alhusseini, D. Blend, K. Dilsiz[85], L. Emediato, G. Karaman, O.K. Köseyan, J.-P. Merlo, A. Mestvirishvili[86], O. Neogi, H. Ogul[87], Y. Onel, A. Penzo, C. Snyder, E. Tiras[88]

Johns Hopkins University, Baltimore, Maryland, USA
B. Blumenfeld, L. Corcodilos, J. Davis, A.V. Gritsan, L. Kang, S. Kyriacou, P. Maksimovic, M. Roguljic, J. Roskes, S. Sekhar, M. Swartz

The University of Kansas, Lawrence, Kansas, USA
A. Abreu, L.F. Alcerro Alcerro, J. Anguiano, S. Arteaga Escatel, P. Baringer, A. Bean, Z. Flowers, D. Grove, J. King, G. Krintiras, M. Lazarovits, C. Le Mahieu, J. Marquez, N. Minafra, M. Murray, M. Nickel, M. Pitt, S. Popescu[89], C. Rogan, C. Royon, R. Salvatico, S. Sanders, C. Smith, G. Wilson

Kansas State University, Manhattan, Kansas, USA
B. Allmond, R. Gujju Gurunadha, A. Ivanov, K. Kaadze, Y. Maravin, J. Natoli, D. Roy, G. Sorrentino

University of Maryland, College Park, Maryland, USA
A. Baden, A. Belloni, J. Bistany-riebman, Y.M. Chen, S.C. Eno, N.J. Hadley, S. Jabeen, R.G. Kellogg, T. Koeth, B. Kronheim, Y. Lai, S. Lascio, A.C. Mignerey, S. Nabili, C. Palmer, C. Papageorgakis, M.M. Paranjpe, L. Wang

Massachusetts Institute of Technology, Cambridge, Massachusetts, USA
J. Bendavid, I.A. Cali, P.c. Chou, M. D'Alfonso, J. Eysermans, C. Freer, G. Gomez-Ceballos, M. Goncharov, G. Grosso, P. Harris, D. Hoang, D. Kovalskyi, J. Krupa, L. Lavezzo, Y.-J. Lee, K. Long, C. Mcginn, A. Novak, C. Paus, D. Rankin, C. Roland, G. Roland, S. Rothman, G.S.F. Stephans, Z. Wang, B. Wyslouch, T. J. Yang

University of Minnesota, Minneapolis, Minnesota, USA
B. Crossman, B.M. Joshi, C. Kapsiak, M. Krohn, D. Mahon, J. Mans, B. Marzocchi, M. Revering, R. Rusack, R. Saradhy, N. Strobbe

University of Mississippi, Oxford, Mississippi, USA
L.M. Cremaldi

University of Nebraska-Lincoln, Lincoln, Nebraska, USA
K. Bloom, D.R. Claes, G. Haza, J. Hossain, C. Joo, I. Kravchenko, J.E. Siado, W. Tabb, A. Vagnerini, A. Wightman, F. Yan, D. Yu

State University of New York at Buffalo, Buffalo, New York, USA
H. Bandyopadhyay, L. Hay, H.w. Hsia, I. Iashvili, A. Kalogeropoulos, A. Kharchilava, M. Morris, D. Nguyen, S. Rappoccio, H. Rejeb Sfar, A. Williams, P. Young

Northeastern University, Boston, Massachusetts, USA
G. Alverson, E. Barberis, J. Dervan, Y. Haddad, Y. Han, A. Krishna, J. Li, M. Lu, G. Madigan, R. Mccarthy, D.M. Morse, V. Nguyen, T. Orimoto, A. Parker, L. Skinnari, D. Wood

Northwestern University, Evanston, Illinois, USA
J. Bueghly, S. Dittmer, K.A. Hahn, Y. Liu, Y. Miao, D.G. Monk, M.H. Schmitt, A. Taliercio, M. Velasco

University of Notre Dame, Notre Dame, Indiana, USA
G. Agarwal, R. Band, R. Bucci, S. Castells, A. Das, R. Goldouzian, M. Hildreth, K.W. Ho, K. Hurtado Anampa, T. Ivanov, C. Jessop, K. Lannon, J. Lawrence, N. Loukas, L. Lutton, J. Mariano, N. Marinelli, I. Mcalister, T. McCauley, C. Mcgrady, C. Moore, Y. Musienko[17], H. Nelson, M. Osherson, A. Piccinelli, R. Ruchti, A. Townsend, Y. Wan, M. Wayne, H. Yockey, M. Zarucki, L. Zygala

The Ohio State University, Columbus, Ohio, USA
A. Basnet, B. Bylsma, M. Carrigan, L.S. Durkin, C. Hill, M. Joyce, M. Nunez Ornelas, K. Wei, B.L. Winer, B. R. Yates

Princeton University, Princeton, New Jersey, USA
H. Bouchamaoui, P. Das, G. Dezoort, P. Elmer, A. Frankenthal, B. Greenberg, N. Haubrich, K. Kennedy, G. Kopp, S. Kwan, D. Lange, A. Loeliger, D. Marlow, I. Ojalvo, J. Olsen, A. Shevelev, D. Stickland, C. Tully

University of Puerto Rico, Mayaguez, Puerto Rico, USA
G. Fidalgo, S. Malik, C. Suarez

Purdue University, West Lafayette, Indiana, USA
A.S. Bakshi, V.E. Barnes, S. Chandra, R. Chawla, A. Gu, L. Gutay, M. Jones, A.W. Jung, A.M. Koshy, M. Liu, G. Negro, N. Neumeister, G. Paspalaki, S. Piperov, V. Scheurer, J.F. Schulte, M. Stojanovic, J. Thieman, A. K. Virdi, F. Wang, W. Xie

Purdue University Northwest, Hammond, Indiana, USA
J. Dolen, N. Parashar, A. Pathak

Rice University, Houston, Texas, USA
D. Acosta, T. Carnahan, K.M. Ecklund, P.J. Fernández Manteca, S. Freed, P. Gardner, F.J.M. Geurts, W. Li, J. Lin, O. Miguel Colin, B.P. Padley, R. Redjimi, J. Rotter, E. Yigitbasi, Y. Zhang

University of Rochester, Rochester, New York, USA

A. Bodek, P. de Barbaro, R. Demina, J.L. Dulemba, A. Garcia-Bellido, O. Hindrichs, A. Khukhunaishvili, N. Parmar, P. Parygin[90], E. Popova[90], R. Taus

The Rockefeller University, New York, New York, USA
K. Goulianos

Rutgers, The State University of New Jersey, Piscataway, New Jersey, USA
B. Chiarito, J.P. Chou, S.V. Clark, D. Gadkari, Y. Gershtein, E. Halkiadakis, M. Heindl, C. Houghton, D. Jaroslawski, O. Karacheban[27], S. Konstantinou, I. Laflotte, A. Lath, R. Montalvo, K. Nash, J. Reichert, H. Routray, P. Saha, S. Salur, S. Schnetzer, S. Somalwar, R. Stone, S.A. Thayil, S. Thomas, J. Vora, H. Wang

University of Tennessee, Knoxville, Tennessee, USA
H. Acharya, D. Ally, A.G. Delannoy, S. Fiorendi, S. Higginbotham, T. Holmes, A.R. Kanuganti, N. Karunarathna, L. Lee, E. Nibigira, S. Spanier

Texas A&M University, College Station, Texas, USA
D. Aebi, M. Ahmad, T. Akhter, O. Bouhali[91], R. Eusebi, J. Gilmore, T. Huang, T. Kamon[92], H. Kim, S. Luo, R. Mueller, D. Overton, D. Rathjens, A. Safonov

Texas Tech University, Lubbock, Texas, USA
N. Akchurin, J. Damgov, N. Gogate, V. Hegde, A. Hussain, Y. Kazhykarim, K. Lamichhane, S.W. Lee, A. Mankel, T. Peltola, I. Volobouev

Vanderbilt University, Nashville, Tennessee, USA
E. Appelt, Y. Chen, S. Greene, A. Gurrola, W. Johns, R. Kunnawalkam Elayavalli, A. Melo, F. Romeo, P. Sheldon, S. Tuo, J. Velkovska, J. Viinikainen

University of Virginia, Charlottesville, Virginia, USA
B. Cardwell, B. Cox, J. Hakala, R. Hirosky, A. Ledovskoy, C. Neu

Wayne State University, Detroit, Michigan, USA
S. Bhattacharya, P.E. Karchin

University of Wisconsin - Madison, Madison, Wisconsin, USA
A. Aravind, S. Banerjee, K. Black, T. Bose, S. Dasu, I. De Bruyn, P. Everaerts, C. Galloni, H. He, M. Herndon, A. Herve, C.K. Koraka, A. Lanaro, R. Loveless, J. Madhusudanan Sreekala, A. Mallampalli, A. Mohammadi, S. Mondal, G. Parida, L. Pétré, D. Pinna, A. Savin, V. Shang, V. Sharma, W.H. Smith, D. Teague, H.F. Tsoi, W. Vetens, A. Warden

Authors affiliated with an institute or an international laboratory covered by a cooperation agreement with CERN
S. Afanasiev, V. Alexakhin, V. Andreev, Yu. Andreev, T. Aushev, M. Azarkin, A. Babaev, V. Blinov[93], E. Boos, V. Borshch, D. Budkouski, V. Bunichev, M. Chadeeva[93], V. Chekhovsky, R. Chistov[93], A. Dermenev, T. Dimova[93], D. Druzhkin[94], M. Dubinin[82], L. Dudko, A. Ershov, G. Gavrilov, V. Gavrilov, S. Gninenko, V. Golovtcov, N. Golubev, I. Golutvin, I. Gorbunov, A. Gribushin, Y. Ivanov, V. Kachanov, V. Karjavine, A. Karneyeu, V. Kim[93], M. Kirakosyan, D. Kirpichnikov, M. Kirsanov, V. Klyukhin, O. Kodolova[95], D. Konstantinov, V. Korenkov, A. Kozyrev[93], N. Krasnikov, A. Lanev, P. Levchenko[96], N. Lychkovskaya, V. Makarenko, A. Malakhov, V. Matveev[93], V. Murzin, A. Nikitenko[97,95], S. Obraztsov, V. Oreshkin, V. Palichik, V. Perelygin,

S. Petrushanko, S. Polikarpov[93], V. Popov, O. Radchenko[93], M. Savina, V. Savrin, V. Shalaev, S. Shmatov, S. Shulha, Y. Skovpen[93], S. Slabospitskii, V. Smirnov, A. Snigirev, D. Sosnov, V. Sulimov, E. Tcherniaev, A. Terkulov, O. Teryaev, I. Tlisova, A. Toropin, L. Uvarov, A. Uzunian, A. Vorobyev†, N. Voytishin, B.S. Yuldashev[98], A. Zarubin, I. Zhizhin, A. Zhokin

†: Deceased
[1]Also at Yerevan State University, Yerevan, Armenia
[2]Also at TU Wien, Vienna, Austria
[3]Also at Institute of Basic and Applied Sciences, Faculty of Engineering, Arab Academy for Science, Technology and Maritime Transport, Alexandria, Egypt
[4]Also at Ghent University, Ghent, Belgium
[5]Also at Universidade do Estado do Rio de Janeiro, Rio de Janeiro, Brazil
[6]Also at Universidade Estadual de Campinas, Campinas, Brazil
[7]Also at Federal University of Rio Grande do Sul, Porto Alegre, Brazil
[8]Also at UFMS, Nova Andradina, Brazil
[9]Also at Nanjing Normal University, Nanjing, China
[10]Now at The University of Iowa, Iowa City, Iowa, USA
[11]Also at University of Chinese Academy of Sciences, Beijing, China
[12]Also at China Center of Advanced Science and Technology, Beijing, China
[13]Also at University of Chinese Academy of Sciences, Beijing, China
[14]Also at China Spallation Neutron Source, Guangdong, China
[15]Now at Henan Normal University, Xinxiang, China
[16]Also at Université Libre de Bruxelles, Bruxelles, Belgium
[17]Also at an institute or an international laboratory covered by a cooperation agreement with CERN
[18]Also at Suez University, Suez, Egypt
[19]Now at British University in Egypt, Cairo, Egypt
[20]Also at Purdue University, West Lafayette, Indiana, USA
[21]Also at Université de Haute Alsace, Mulhouse, France
[22]Also at Department of Physics, Tsinghua University, Beijing, China
[23]Also at The University of the State of Amazonas, Manaus, Brazil
[24]Also at University of Hamburg, Hamburg, Germany
[25]Also at RWTH Aachen University, III. Physikalisches Institut A, Aachen, Germany
[26]Also at Bergische University Wuppertal (BUW), Wuppertal, Germany
[27]Also at Brandenburg University of Technology, Cottbus, Germany
[28]Also at Forschungszentrum Jülich, Juelich, Germany
[29]Also at CERN, European Organization for Nuclear Research, Geneva, Switzerland
[30]Also at Institute of Physics, University of Debrecen, Debrecen, Hungary
[31]Also at Institute of Nuclear Research ATOMKI, Debrecen, Hungary
[32]Now at Universitatea Babes-Bolyai - Facultatea de Fizica, Cluj-Napoca, Romania
[33]Also at MTA-ELTE Lendület CMS Particle and Nuclear Physics Group, Eötvös Loránd University, Budapest, Hungary
[34]Also at HUN-REN Wigner Research Centre for Physics, Budapest, Hungary
[35]Also at Physics Department, Faculty of Science, Assiut University, Assiut, Egypt
[36]Also at Punjab Agricultural University, Ludhiana, India
[37]Also at University of Visva-Bharati, Santiniketan, India
[38]Also at Indian Institute of Science (IISc), Bangalore, India
[39]Also at IIT Bhubaneswar, Bhubaneswar, India
[40]Also at Institute of Physics, Bhubaneswar, India

[41]Also at University of Hyderabad, Hyderabad, India
[42]Also at Deutsches Elektronen-Synchrotron, Hamburg, Germany
[43]Also at Isfahan University of Technology, Isfahan, Iran
[44]Also at Sharif University of Technology, Tehran, Iran
[45]Also at Department of Physics, University of Science and Technology of Mazandaran, Behshahr, Iran
[46]Also at Department of Physics, Isfahan University of Technology, Isfahan, Iran
[47]Also at Italian National Agency for New Technologies, Energy and Sustainable Economic Development, Bologna, Italy
[48]Also at Centro Siciliano di Fisica Nucleare e di Struttura Della Materia, Catania, Italy
[49]Also at Università degli Studi Guglielmo Marconi, Roma, Italy
[50]Also at Scuola Superiore Meridionale, Università di Napoli 'Federico II', Napoli, Italy
[51]Also at Fermi National Accelerator Laboratory, Batavia, Illinois, USA
[52]Also at Consiglio Nazionale delle Ricerche - Istituto Officina dei Materiali, Perugia, Italy
[53]Also at Department of Applied Physics, Faculty of Science and Technology, Universiti Kebangsaan Malaysia, Bangi, Malaysia
[54]Also at Consejo Nacional de Ciencia y Tecnología, Mexico City, Mexico
[55]Also at Trincomalee Campus, Eastern University, Sri Lanka, Nilaveli, Sri Lanka
[56]Also at Saegis Campus, Nugegoda, Sri Lanka
[57]Also at National and Kapodistrian University of Athens, Athens, Greece
[58]Also at Ecole Polytechnique Fédérale Lausanne, Lausanne, Switzerland
[59]Also at Universität Zürich, Zurich, Switzerland
[60]Also at Stefan Meyer Institute for Subatomic Physics, Vienna, Austria
[61]Also at Laboratoire d'Annecy-le-Vieux de Physique des Particules, IN2P3-CNRS, Annecy-le-Vieux, France
[62]Also at Near East University, Research Center of Experimental Health Science, Mersin, Turkey
[63]Also at Konya Technical University, Konya, Turkey
[64]Also at Izmir Bakircay University, Izmir, Turkey
[65]Also at Adiyaman University, Adiyaman, Turkey
[66]Also at Bozok Universitetesi Rektörlügü, Yozgat, Turkey
[67]Also at Marmara University, Istanbul, Turkey
[68]Also at Milli Savunma University, Istanbul, Turkey
[69]Also at Kafkas University, Kars, Turkey
[70]Now at stanbul Okan University, Istanbul, Turkey
[71]Also at Hacettepe University, Ankara, Turkey
[72]Also at Erzincan Binali Yildirim University, Erzincan, Turkey
[73]Also at Istanbul University - Cerrahpasa, Faculty of Engineering, Istanbul, Turkey
[74]Also at Yildiz Technical University, Istanbul, Turkey
[75]Also at Vrije Universiteit Brussel, Brussel, Belgium
[76]Also at School of Physics and Astronomy, University of Southampton, Southampton, United Kingdom
[77]Also at IPPP Durham University, Durham, United Kingdom
[78]Also at Monash University, Faculty of Science, Clayton, Australia
[79]Also at Università di Torino, Torino, Italy
[80]Also at Bethel University, St. Paul, Minnesota, USA
[81]Also at Karamanoğlu Mehmetbey University, Karaman, Turkey
[82]Also at California Institute of Technology, Pasadena, California, USA
[83]Also at United States Naval Academy, Annapolis, Maryland, USA

[84]Also at Ain Shams University, Cairo, Egypt
[85]Also at Bingol University, Bingol, Turkey
[86]Also at Georgian Technical University, Tbilisi, Georgia
[87]Also at Sinop University, Sinop, Turkey
[88]Also at Erciyes University, Kayseri, Turkey
[89]Also at Horia Hulubei National Institute of Physics and Nuclear Engineering (IFIN-HH), Bucharest, Romania
[90]Now at an institute or an international laboratory covered by a cooperation agreement with CERN
[91]Also at Texas A&M University at Qatar, Doha, Qatar
[92]Also at Kyungpook National University, Daegu, Korea
[93]Also at another institute or international laboratory covered by a cooperation agreement with CERN
[94]Also at Universiteit Antwerpen, Antwerpen, Belgium
[95]Also at Yerevan Physics Institute, Yerevan, Armenia
[96]Also at Northeastern University, Boston, Massachusetts, USA
[97]Also at Imperial College, London, United Kingdom
[98]Also at Institute of Nuclear Physics of the Uzbekistan Academy of Sciences, Tashkent, Uzbekistan